

# Beyond coastal hazards: A comprehensive methodology for the assessment of climate-related hazards in European coastal cities

Emilio Laino<sup>a</sup>, Gregorio Iglesias<sup>a,b,\*</sup>

<sup>a</sup> School of Engineering and Architecture & Environmental Research Institute, MaREI, University College Cork, Cork, Ireland

<sup>b</sup> University of Plymouth, School of Engineering, Computing and Mathematics, Marine Building, Drake Circus, United Kingdom

## ARTICLE INFO

### Keywords:

Climate change extreme impacts  
Coastal flooding  
Coastal erosion  
Coastal cities  
Multi-hazard assessment  
Risk assessment

## ABSTRACT

As climate change intensifies, European coastal cities face escalating risks from multiple climate-related hazards. Addressing these challenges requires capturing the multifaceted nature of climate risks adequately. This paper presents a novel multi-hazard risk assessment methodology for European coastal cities, which integrates indicators of hazard, exposure, sensitivity, and adaptive capacity. It advances beyond existing models by incorporating a wide array of climate-related hazards and significant indicators. Applied to six diverse coastal cities across different climatic zones and urbanization levels, the methodology proves robust and versatile, offering a comprehensive approach to understanding climate risks. Findings reveal that Varna has the lowest hazard score compared to other cities. Cork and Viana do Castelo are significantly affected by coastal hazards, while La Spezia exhibits very low coastal hazard scores but high land hazard scores. The exposure component ranges between medium and low values, with a maximum in Klaipeda and a minimum in Viana do Castelo. In terms of vulnerability, Viana do Castelo and Bergen stand out, while Cork exhibits the lowest score. Finally, risk presents a balanced landscape, where cities with the highest scores in hazard and exposure also exhibit the lowest levels of vulnerability and vice versa. The discussion on policy implications advocates for participatory resilience-building, leveraging new technologies and non-traditional indicators to enhance urban adaptive capacity. The granularity and specificity inherent to the proposed methodology offer a tool to compare and identify high-risk cities systematically, allowing for a more informed and targeted approach to resilience building and strategic allocation of often limited resources.

## 1. Introduction

In the face of escalating climate change impacts (Bergillos et al., 2020; Costa et al., 2023; Li et al., 2021; Vousdoukas et al., 2020; Zscheischler et al., 2018), multi-hazard risk assessments (MHRA) have become essential to understanding and mitigating the diverse threats posed by climate-related hazards (Elliott et al., 2014; Hu et al., 2023; Koks et al., 2019; McEvoy et al., 2021). These assessments typically employ index-based approaches, recognized for their robustness in calculating risk as a function of hazard, exposure, and vulnerability, in line with recommendations from the Intergovernmental Panel on Climate Change (Williams et al., 2018). A variety of models and frameworks have been developed to address these challenges, each offering distinct methodologies and insights (Gallina et al., 2016; Owolabi and Sajjad, 2023; Tang et al., 2013).

Globally recognized models, such as CLIMADA by ETH Zurich and

the DIVA model from the Global Climate Forum, constitute benchmarks in this field. CLIMADA integrates hazard, exposure, and vulnerability data to quantify and monetize natural disaster impacts (Aznar-Siguan and Bresch, 2019), while DIVA focuses on the socio-economic and biophysical consequences of sea-level rise and socio-economic development (Fang et al., 2020; Hinkel and Klein, 2009). Additionally, DELTARES models provide invaluable insights into coastal dynamics and flood risk management through detailed physical simulations – methodologies highly relevant to the European coastal context.

Specifically tailored to European coastal cities, EUROSION offers detailed analyses of coastal erosion processes, providing essential guidelines for coastal zone management in Europe. Costs from diverse hazards are assessed in the ConHaz project. The focus on urban climate change adaptation and mitigation of the RAMSES Project, including cost-benefit analysis tools, is particularly relevant for city planners. Moreover, initiatives like the BRANCH Project and the OPERR framework address biodiversity impacts and ecological forecasting, including

\* Corresponding author. School of Engineering and Architecture & Environmental Research Institute, MaREI, University College Cork, Cork, Ireland.

E-mail address: [gregorio.iglesias@ucc.ie](mailto:gregorio.iglesias@ucc.ie) (G. Iglesias).

<https://doi.org/10.1016/j.ocecoaman.2024.107343>

Received 30 April 2024; Received in revised form 8 July 2024; Accepted 15 August 2024

Available online 20 August 2024

0964-5691/© 2024 The Authors. Published by Elsevier Ltd. This is an open access article under the CC BY license (<http://creativecommons.org/licenses/by/4.0/>).

### Acronyms

|         |  |
|---------|--|
| C3S CDS | Copernicus Climate Change Service Climate Data Store |
| EDO     | European Drought Observatory                         |
| ESL     | Extreme Sea Level                                    |
| GDP     | Gross Domestic Product                               |
| IPCC    | Intergovernmental Panel on Climate Change            |
| JRC     | Joint Research Centre                                |
| LECZ    | Low-Elevation Coastal Zone                           |
| LULC    | Land Use and Land Cover                              |
| MMU     | Minimum Mapping Unit                                 |
| MSL     | Mean Sea Level                                       |
| OSM     | OpenStreetMap  |

riverine discharges – essential aspects of coastal management in Europe. The European Climate Adaptation Platform (Climate-ADAPT) and the ESMERALDA Project further enrich this landscape by offering resources for climate adaptation planning and ecosystem services assessment, which are crucial for holistic urban and environmental planning in coastal areas.

Amidst these advancements, the SCORE project emerges as a pivotal initiative, aiming to co-create climate change adaptation and resilience strategies in coastal cities (Laino and Iglesias, 2023a; Tiwari et al., 2022). This endeavour is achieved through collaborative participation between public institutions, research centres, decision-making, and operational bodies, all centred around the novel concept of the Coastal City Living Lab. This approach to tackling the challenges posed by climate change, especially in terms of sea-level rise and climate-related hazards, necessitates effective communication and decision-support tools (Kerguillec et al., 2019). Such tools are crucial for fostering collaboration among stakeholders, enabling informed decision-making and the development of innovative solutions tailored to the unique dynamics of coastal urban environments (Elrick-Barr et al., 2024; McKinley et al., 2021; Measham et al., 2011).

In this context, academic research offers noteworthy examples of approaches addressing multiple climate-related hazards in Europe. Lung et al. (2013) combined indicators of climatic and non-climatic change to assess regional-level impacts in Europe. Their indicator-based framework integrates climate models with socio-economic data to quantify changes in heat-related, river flooding and forest fire hazards. Crespi et al. (2020) offer a comprehensive analysis of climate-related hazard indices in Europe, selecting 32 indices using a wide array of data from the Copernicus Climate Change Service Climate Data Store (C3S CDS), including E-OBS (daily gridded observation dataset over Europe), ERA5 (fifth generation ECMWF atmospheric reanalysis of the global climate), ERA5-Land (enhanced resolution ERA5 for land variables), UERRA (regional reanalysis of near-surface variables for Europe), CMIP5 (fifth phase of the Coupled Model Inter-comparison Project), CORDEX (regional climate model data for Europe), and other key index datasets described in the report. The methodical approach in compiling and analysing these indices provides a solid foundation for future research on climate-related hazards in Europe. Hincks et al. (2023) develop a new typology of climate risk at NUTS3 level under the call of IPCC for sub-national climate change risk awareness. They use K-means clustering to analyse 49 variables, creating a detailed classification that highlights the varying climate change risks across Europe.

In the international context, Binita et al. (2021) developed a climate risk index for the United States at the county level for some climate-related hazards. They combined high-resolution downscaled climate projections and indicators of exposure and vulnerability to estimate future climate risks for planning and implementing targeted adaptation strategies at the local level. Tiepolo et al. (2019) emphasize the importance of combining local and scientific knowledge in assessing

multi-hazard risks in Mauritania. Their approach integrates community input with scientific data to assess risks and propose appropriate risk treatment actions. Araya-Muñoz et al. (2017) and Pourghasemi et al. (2019) further contribute to the methodological diversity in this field, highlighting the benefits of innovative and data-driven approaches. The former uses spatial fuzzy logic modelling to assess multiple hazards in Chile, while the latter develops a multi-hazard probability map for Iran using a novel ensemble model.

The increasing impacts of climate change necessitate comprehensive multi-hazard risk assessments (MHRA) to understand and mitigate the diverse threats posed by climate-related hazards. While numerous studies have focused on climate-related indices in Europe, a significant gap remains in the development of cross-regional methodologies that address the full spectrum of climate-related hazards, particularly in coastal cities (Kappes et al., 2012; Laino et al., 2024; Owolabi and Sajjad, 2023). These cities, which are central to societal and economic well-being, face compounded risks where land and coastal hazards converge, further exacerbated by climate change (Beden and Ulke, 2020; Colten et al., 2022; Espinosa et al., 2022; Toledo et al., 2022). Current models and frameworks provide valuable insights but do not fully address the unique dynamics of coastal urban environments. Additionally, there is a notable lack of cross-regional comparative studies, which limits the ability to benchmark and implement targeted interventions across different coastal cities (Laino et al., 2024). Effective risk assessment and management in these coastal regions are critical yet challenging.

In this context, this study sets out with several research objectives. It aims to provide a set of critical climate-related indicators necessary for a comprehensive multi-hazard risk assessment in European coastal cities, covering a wide variety of climate-related hazards. The methodology involves leveraging a rich array of indicators for hazard, exposure, and vulnerability in a systematic and standardized approach that builds on current risk assessment practices and facilitates more effective climate adaptation strategies. Furthermore, it is designed to allow for comparative baseline analysis across European coastal cities, providing a unique opportunity for benchmarking and collaborative resilience-building efforts (Glavovic et al., 2022; Wright et al., 2015). To demonstrate its applicability and effectiveness in varied regional contexts, the proposed methodology is tested in six diverse European coastal cities, contributing reliable insights across different urban environments. The ultimate goal is to form the foundation for a decision-support tool designed for policymakers and urban planners, enabling them to prioritize coastal management actions based on the severity and urgency of the specific risks faced by each city.

## 2. Materials and methods

### 2.1. Risk framework

In this study, the conception of risk follows the risk assessment framework developed by the Intergovernmental Panel on Climate Change (IPCC) (IPCC, 2014). At the core of this framework is the concept that risk is a function of hazard, exposure, and vulnerability. Hazards refer to climate-related physical events or trends, such as extreme weather events or long-term shifts in climate patterns. Exposure denotes the presence of populations, ecosystems, or assets in places that could be adversely affected by these hazards. Vulnerability involves the sensitivity and adaptive capacity of these systems, highlighting their propensity to suffer harm. This paradigm is applied here by developing a series of indicators that capture the different elements of risk, allowing for a detailed and systematic evaluation of diverse climate-related threats. By systematically integrating these elements, the framework provides a structured approach to risk assessment, enabling policymakers and stakeholders to prioritize actions that enhance resilience and reduce vulnerability to climate change. Fig. 1 illustrates the relationship between the indicators developed in this study and their

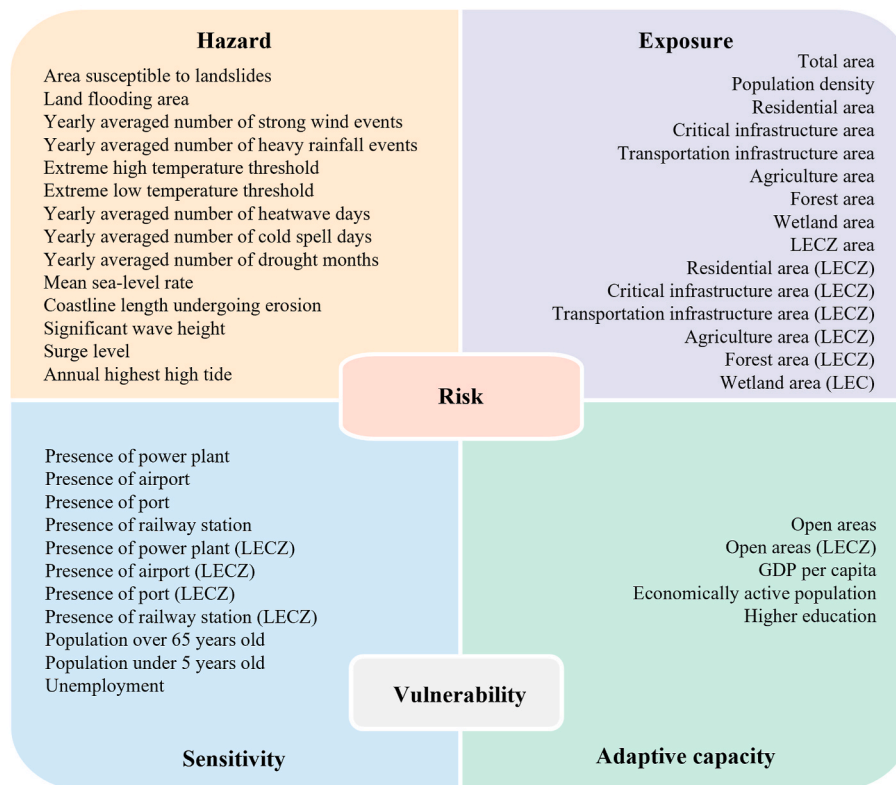


Fig. 1. Relationship between developed indicators and corresponding risk parameters.

corresponding risk parameters, which is detailed hereinafter.

### 2.2. Selection of indicators

The indicators for developing the MHRA were devised by means of a methodological framework designed to ensure robustness, relevance, and operational practicality. This framework was built on the pillars of comprehensive literature review, local engagement, and stringent evaluation criteria addressing both conceptual and technical aspects. Each step in the selection process was informed by the overarching goal to effectively measure and interpret climate-related hazards, taking into account the inherent complexities and specificities in the context of coastal cities across Europe.

A thorough review of academic literature, policy documents, and grey literature was conducted to gather a broad spectrum of perspectives on the risk elements including hazard, exposure, sensitivity, and adaptive capacity (Laino and Iglesias, 2023b, 2023c). Data sources were evaluated for their credibility, relevance, and compatibility with the objectives of the study. This involved an assessment of data repositories at both European and international levels to ensure comprehensive coverage.

Engagement with local expertise through the SCORE project was integral to the process, ensuring that the selection of indicators resonated with the practical needs and insights of those actively involved in climate risk management (Laino and Iglesias, 2023a; Paranunzio et al., 2024). Workshops and meetings provided platforms for discourse, allowing for the refinement of the role of the new methodology, methodological development, and the contextualization of future outputs.

Conceptual relevance was a primary criterion, ensuring that each selected indicator aligned effectively with the identified risk themes: hazard, exposure, sensitivity, and adaptive capacity. Technical robustness was assessed based on several parameters including data availability at the required spatial unit (e.g., city-scale), clarity and comparability of definitions, transparency in data collection methods,

continuity in methodologies, relevance, and the presence of appropriate time series data.

The definition of thresholds, whether fixed or percentile-based, was carefully considered, acknowledging the advantages and drawbacks of each approach. The temporal and spatial resolution of data was aligned with the characteristic scales of the climate-related hazards under study, ensuring that the indices could effectively capture and represent localized and short-term hazard events.

The complexity involved in computing each indicator was evaluated, with a preference for indices that, while comprehensive, remained interpretable and feasible in terms of data requirements. The robustness of each index was critically assessed, taking into account uncertainties in threshold choices, model data, and the practical implications of spatial resolution mismatches.

The operationalization of indices was tailored to specific applications and end-user requirements. This involved thoughtful considerations regarding the choice of reference periods, climate scenarios, and visualization elements. The selection process was dynamic, allowing for adjustments and refinements to ensure that the indices remained relevant and practical for policymaking, planning, and climate risk mitigation efforts.

### 2.3. Study cases

Six diverse coastal cities were selected representatives of different climate zones, seas, existing academic results, degree of urbanization and Gross Domestic Products (GDP). The geographic characterization of selected coastal cities was conducted using a combination of datasets. The extents of urban areas were delineated utilizing the Urban Atlas 2012 dataset, which provides detailed land use and land cover data across European cities. This dataset was employed to define the city extents, aligning them with the respective administrative boundaries. For the cities of Bergen, Klaipeda, La Spezia, and Viana do Castelo, the city extents were matched with their municipality-level boundaries. In

the cases of Cork (reflecting the pre-2019 administrative structure) and Varna, the extents were aligned with the boundaries defined at the city council level.

The Low-Elevation Coastal Zone (LECZ) – land located below 10 m and contiguous to the sea – was delineated using the high-resolution MERIT DEM (MacManus et al., 2021; Yamazaki et al., 2017), identifying areas most exposed to coastal hazards. Specific coordinate points were sourced from OpenStreetMap (OSM), a comprehensive open-source mapping platform, for later calculations. The retrieval of these coordinates was facilitated by the geopy library, a Python-based toolset designed for geocoding, which enabled efficient extraction and manipulation of geospatial data from OSM. This integration of datasets provided a robust framework for the comprehensive geographic characterization of the selected coastal cities, as depicted in Fig. 2.

#### 2.4. Climate-related hazards indicators

The methodology is characterised for evaluating a comprehensive suite of climate-related hazards. These hazards, which are outlined in Table 1, encompass sea-level rise, coastal and land flooding, coastal erosion, heavy rainfall, droughts, extreme temperatures, heatwaves,

cold spells, strong winds, and landslides. The indicators are the result of integrating insights from leading sources and contemporary studies, specifically designed for the European setting (Laino and Iglesias, 2024). Initially, the Sixth Assessment Report by the IPCC was utilized as a key document (Ranasinghe et al., 2021), presenting a detailed categorization of climate-related phenomena, which lays the groundwork for recognizing potential threats to coastal areas.

Subsequently, the process of refining the indicators was guided by insights from the European Topic Centre on Climate Change Impacts, Vulnerability, and Adaptation. This body assesses and ranks climate hazard indices for Europe, considering their importance, relevance to adaptation, availability of data, and the reliability of that data (Crespi et al., 2020). The goal is to develop indicators that are uniformly and systematically applicable to the European coastal context.

The methodology is also informed by and contributes to recent research that utilizes hazard indicators. Studies by Lung et al. (2013) and Hincks et al. (2023) examine various hazards such as coastal threats, extreme temperatures, precipitation events, floods, droughts, and landslides for regional risk evaluations in Europe. The recent study by Laino and Iglesias (2023c), which merges a review of the existing literature with feedback from stakeholders in the target cities, offers

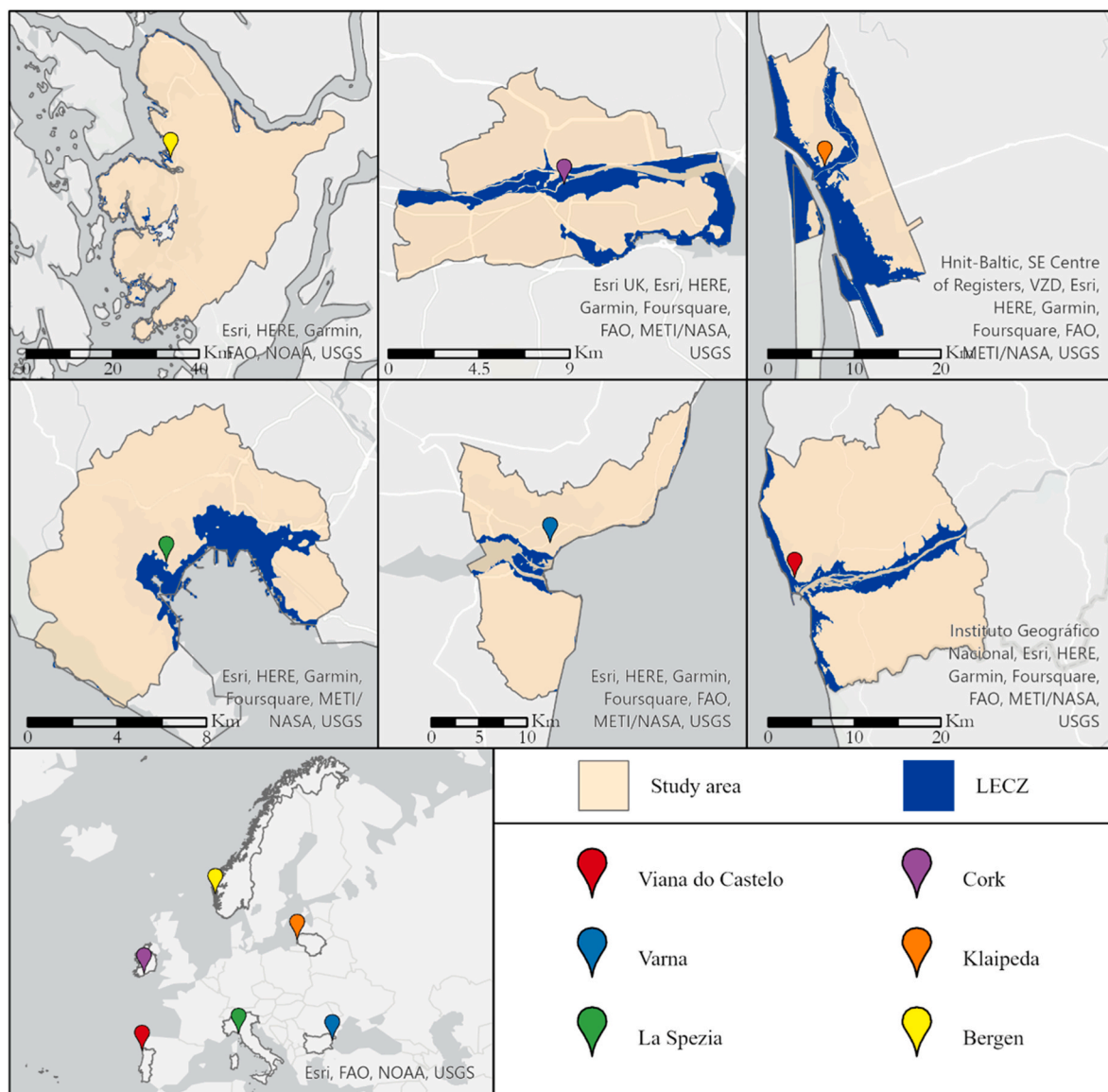


Fig. 2. Study areas, including city boundary and low-elevation coastal zone. Data source: OpenStreetMap, Urban Atlas 2012 and Yamazaki et al. (2017).

**Table 1**  
Indicators assessing the risk component of hazard, including spatial and temporal resolution and data source.

| Indicator (units)                              | Spatial resolution and coverage         | Temporal resolution and coverage  | Data source   |
|--|---|---|---|
| <b>MSL rate (mm/year)</b>                      | 1-degree grid; global                   | 2020 decade relative to a 1995–2014 baseline  | NASA Sea-Level Projection Tool (Garner et al., 2021; Intergovernmental Panel on Climate Change, 2023; Kopp et al., 2023)                      |
| <b>Storm surge level (m)</b>                   | 0.1-degree grid; Europe                 | Value corresponding to the 50th percentile of the 50-year return period from 2001 to 2017 ERA5 reanalysis | Indicators of water level change for European coasts in the 21st Century (Caires and Yan, 2020; Hersbach et al., 2020; Yan et al., 2020)      |
| <b>Significant wave height (m)</b>             | 0.1-degree grid; Europe                 | Average value between the 90th and 100th percentiles from 2001 to 2017 ERA5 reanalysis                    | Indicators of water level change for European coasts in the 21st Century Wave (Caires and Yan, 2020; Hersbach et al., 2020; Yan et al., 2020) |
| <b>Peak wave period (s)</b>                    | 0.1-degree grid; Europe                 | Average value between the 90th and 100th percentiles from 2001 to 2017 ERA5 reanalysis                    | Indicators of water level change for European coasts in the 21st Century Wave (Caires and Yan, 2020; Hersbach et al., 2020; Yan et al., 2020) |
| <b>Annual highest high tide (m)</b>            | 0.1-degree grid; Europe                 | Value corresponding to the 50th percentile of the 50-year return period from 2001 to 2017 ERA5 reanalysis | Indicators of water level change for European coasts in the 21st Century Wave (Caires and Yan, 2020; Hersbach et al., 2020; Yan et al., 2020) |
| <b>Coastline length undergoing erosion (%)</b> | 200 m; Europe                           | Single values reflecting conditions up to the early 2000s   | EuroSION (Lenôtre et al., 2004)   |
| <b>Land flooding area (%)</b>                  | 100 m; Europe and its surrounding areas | Values for the 100-year return period based on daily river flows between 1990 and 2016                    | River flood hazard maps for Europe and the Mediterranean Basin region (Dottori et al., 2021)  |
| <b>Heavy rainfall frequency (day/year)</b>     | 0.25-degree; Europe                     | Day; 1981–2019  | Extreme precipitation risk indicators for Europe and European cities from 1950 to 2019 (Hersbach et al., 2020; Mercogliano et al., 2021)      |
| <b>Drought frequency (month/year)</b>          | 1-degree; global                        | Month; 1981–2020  | Global Drought Observatory (European Commission and Joint Research Centre (JRC), 2021)  |
| <b>Extreme high temperature threshold (°C)</b> | 0.25-degree; Europe                     | Day; 1981–2020  | European Drought Observatory (Lavaysse et al., 2018)  |
| <b>Extreme low temperature threshold (°C)</b>  | 0.25-degree; Europe                     | Day; 1981–2020  | European Drought Observatory (Lavaysse et al., 2018)  |
| <b>Heatwave frequency (day/year)</b>           | 0.25-degree; Europe                     | Day; 1981–2020  | European Drought Observatory (Lavaysse et al., 2018)  |
| <b>Cold spell frequency (day/year)</b>         | 0.25-degree; Europe                     | Day; 1981–2020  | European Drought Observatory (Lavaysse et al., 2018)  |

**Table 1 (continued)**

| Indicator (units)                          | Spatial resolution and coverage                        | Temporal resolution and coverage             | Data source  |
|--|--|--|--|
| <b>Strong winds frequency (event/year)</b> | 1 km; 20W-35E, 35N-70N regular latitude-longitude grid | Hour; 1981–2020                              | Winter windstorm indicators for Europe from 1979 to 2021 derived from reanalysis (Copernicus Climate Change Service and Climate Data Store, 2022; Hersbach et al., 2020) |
| <b>Landslide-prone area (%)</b>            | 200 m; Europe  | Single values reflecting conditions pre-2018 | ELsus v2 (Wilde et al., 2018)  |

essential perspectives on local views of climate-related risks. This methodology ensures that the approach is anchored in the most recent scientific findings while also catering to the unique challenges and concerns of coastal cities in climate change adaptation.

Sea-level rise rates for 2020 were estimated using the NASA Sea-Level Projection Tool against a 1995–2014 baseline within the SSP2-4.5 scenario (Garner et al., 2021; Intergovernmental Panel on Climate Change, 2023; Kopp et al., 2023). Extreme sea-level events, crucial for coastal flooding analysis (Almar et al., 2021; Hay et al., 2015; Kulp and Strauss, 2019; Wahl et al., 2017), were characterized by the significant wave height (Hs), the storm surge level and the annual highest high astronomical tide, based on their probability distributions derived from the ERA5 reanalysis dataset (Caires and Yan, 2020; Hersbach et al., 2020; Yan et al., 2020). The proportion of coastline experiencing erosion was determined with data from the EuroSION project, considering the total coastline length (Lenôtre et al., 2004). For pluvial flooding, annual average precipitation events exceeding a 20 mm threshold were averaged from the dataset “Extreme precipitation risk indicators for Europe and European cities from 1950 to 2019” (Mercogliano et al., 2021). River flooding was estimated by quantifying the extents associated with the centennial return period, informed by dataset “River flood hazard maps for Europe and the Mediterranean Basin region” (Dottori et al., 2021). Meteorological drought hazard was evaluated using the SPI-3 index (McKee et al., 1993), identifying monthly values below  $-1$  throughout the 1991–2020 period (WMO, 2012). The assessment of extreme temperatures involved percentile-based thresholds (99th for high and 1st for low) from daily temperature records during key seasonal windows for the baseline period 1981–2000 (Crespi et al., 2020). Heatwaves and cold spells were quantified by the annual average of days from the periods of at least three consecutive days when the daily maximum or minimum temperature exceeded the previous extreme temperature thresholds (Crespi et al., 2020). Storm impact was studied through the annual frequency of strong wind gusts (defined as the maximum 3 s 10 m wind gusts over a 72-h period) exceeding 20 m/s, reflecting the North Atlantic storm influence, based on data from the ERA5 reanalysis from C3S CDS (Copernicus Climate Change Service and Climate Data Store, 2022; Hersbach et al., 2020). Landslide susceptibility was estimated based on the ELSUS v2 dataset, focusing on areas classified as ‘high’ or ‘very high’ in susceptibility. These areas were computed and expressed as a percentage of the total city area. While these indicators provide robust measures for various climate-related hazards, it is important to note that they do not fully capture the entirety of each hazard. The complexity and multifaceted nature of climate-related risks mean that some aspects may not be fully represented by the selected indicators.

## 2.5. Land cover and land use indicators

Land use and land cover (LULC) indicators are widely recognized for

providing fundamental insights into the physical, environmental, and socioeconomic aspects of coastal cities, which are essential for a comprehensive risk assessment (Alessandrini et al., 2024; Magarotto et al., 2017; Wang, 2024). LULC distribution has been thoroughly investigated utilizing the Urban Atlas 2012 dataset (Copernicus Land Monitoring Service, 2012), due to its comprehensive coverage of European cities, regular updates, and a level of precision deemed appropriate for this study. Urban Atlas classifies cities in 17 urban classes with a Minimum Mapping Unit (MMU) of 0.25 ha and 10 Rural Classes with a MMU of 1 ha in 2012, with high thematic accuracy.

For tailoring this dataset to the risk assessment framework, we reclassified the default categories in Urban Atlas. This reclassification involved accounting for areas covered by residential uses, critical infrastructure, agriculture, open spaces, natural vegetation, wetlands, water bodies and other miscellaneous uses. These area calculations were executed for both the entire study region and the LECZs to generate standardized indicators allowing for cross-city comparisons. The computed areas are expressed as percentages of the total city area or the LECZ, respectively. The indicators are compiled in Table 2, detailing their respective contributions to risk.

## 2.6. Presence of critical infrastructure elements

In the realm of disaster risk assessment, the spatial distribution of critical infrastructure within hazard-prone areas is a paramount factor for determining urban sensitivity (Klein and Nicholls, 1999). Examples of common elements which are essential for the functioning of a city include, but are not limited to, hospitals, educational centres, water treatment facilities, public buildings, cultural heritage sites, and emergency services. A high concentration of such infrastructure signifies heightened sensitivity since any damage or disruption can lead to significant detriments to societal functions (Rodriguez-Delgado et al., 2020). In developing a methodology tailored to coastal cities, it is a reasonable assumption that these locales encompass the majority, if not all, of these critical infrastructure elements.

Nevertheless, it is crucial to identify that certain critical infrastructure components, such as power generation plants, ports, airports, and railway stations, may not be as uniformly present across coastal cities. The occurrence and operational capacity of these elements vary considerably and can profoundly influence the risk profile of cities (Chang et al., 2013; Pal et al., 2023; Pant et al., 2016). The presence of these less ubiquitous yet highly significant infrastructural components have been evaluated for each city under study, both for the total city area and the LECZ, providing a set of indicators for sensitivity within the risk analysis framework. Data on the location and spread of such infrastructure has been retrieved from OSM. The indicators consist of a series of binary variables that indicate the presence or absence of a power plant, airport, port, and railway station within the total city area and the LECZ. These indicators are integral to understanding the potential impact of disasters on critical urban systems and the cascading effects on the broader socio-economic landscape.

## 2.7. Socioeconomic indicators

Socioeconomic indicators are fundamental in the context of risk assessment, particularly within coastal urban environments, where the interplay of human and environmental factors is most pronounced (Lückenköter et al., 2013). These indicators provide critical insights into the demographic composition, economic stability, and social infrastructure of communities, factors that collectively define the vulnerability and adaptive capacity of urban populations to climate-related hazards. Population density, age distribution, workforce engagement, and educational attainment are among the key variables that influence the resilience of communities, shaping their ability to prepare for, respond to, and recover from adverse climatic events. Inclusion of these indicators in risk assessment frameworks allows for a

**Table 2**

Indicators relating to land cover and land uses measured over total city area and LECZ.

| Indicator                            | Units | Coverage   | Parameter of risk                 | UA coding                                   |
|--------------------------------------|-------|--|-----------------------------------|---|
| <b>Residential area</b>              | %     | Areas with predominant residential use   | Exposure                          | 11100, 11210, 11220, 11230, 11240 and 11300 |
| <b>Open areas</b>                    | %     | Green urban areas, sports and leisure facilities and open spaces with little or no vegetation  | Vulnerability (adaptive capacity) | 14100, 14200, 33000                         |
| <b>Transportation infrastructure</b> | %     | Areas associated to road, railway, port and airport infrastructure   | Exposure                          | 12210, 12220, 12230, 12300 and 12400        |
| <b>Other critical infrastructure</b> | %     | Healthcare facilities, water and wastewater treatment plants, communication infrastructure, power plants, emergency services, military facilities, educational institutions, cultural heritage sites, industrial and commercial areas and other public, and private services not related to the transport system | Exposure                          | 12100                                       |
| <b>Agricultural area</b>             | %     | Areas with predominant agricultural use  | Exposure                          | 21000, 22000, 23000 and 24000               |
| <b>Natural vegetation area</b>       | %     | Forest and herbaceous vegetation associations  | Exposure                          | 31000 and 32000                             |
| <b>Wetland area</b>                  | %     | Inland and coastal wetlands.   | Exposure                          | 40000                                       |
| <b>Water bodies</b>                  | %     | Sea, lakes, fish ponds, rivers and canals.   | Exposure                          | 50000                                       |
| <b>Other areas</b>                   | %     | Mineral extraction, dumping sites and construction sites and land without current use.   | Not scored                        | 13100, 13300 and 13400                      |

nanced analysis that goes beyond environmental parameters, offering a holistic view of risk that encompasses the socio-economic intricacies of affected populations. This approach ensures that risk mitigation strategies are not only technically sound but also socially inclusive, aligning closely with the real-world complexities and needs of the communities at the forefront of climate change impacts.

In this study, Eurostat, a principal statistical office of the European Union, was selected as the primary data source for analysing demographic and economic indicators of coastal cities (Table 3). By employing the most recent Eurostat data, this study benefits from the methodological rigor, extensive geographic coverage, and standardized data collection methods, ensuring that the socioeconomic indicators are robust, comparable, and reflective of the current state. These indicators, when analysed collectively, provide a comprehensive picture of the

**Table 3**  
Indicators of socioeconomic activity assessed over the total city area.

| Indicator name                 | Short description   | Parameter of risk                 | Variables from Eurostat employed   |
|--------------------------------|---|-----------------------------------|--|
| Population density             | Total city population for a specific year over city area, expressed as inhabitants per squared kilometre.   | Exposure                          | DE1001V: Population on the 1st of January, total   |
| Population under 5 years old   | Population under 5 years old for a specific year, expressed as a percentage of the total population for the same year.  | Vulnerability (sensitivity)       | DE1040V: Population on the 1st of January, 0–4 years, total;   |
| Population over 65 years old   | Population over 65 years old for a specific year, expressed as a percentage of the total population for the same year.  | Vulnerability (sensitivity)       | DE1028V: Population on the 1st of January, 65–74 years, total. DE1055V: Population on the 1st of January, 75 years and over, total |
| Economically active population | Persons that are either employed or unemployed and not part of the economically inactive population for a specific year, which covers all residents over 15 who are not economically active, expressed as a percentage of the total population for the same year. | Vulnerability (adaptive capacity) | EC1001V: Economically active population, total   |
| Unemployment                   | Total population under unemployment, expressed as a percentage over total population.   | Vulnerability (sensitivity)       | EC1010V: Persons unemployed, total   |
| Higher education               | Population with high educational background for a specific year, expressed as a percentage of the total population for the same year.   | Vulnerability (adaptive capacity) | TE2031V: Persons aged 25–64 with ISCED level 5, 6, 7 or 8 (from 2014 onwards) as the highest level of education                    |
| GDP per capita                 | GDP per capita at market prices, measured at NUTS3 level  | Vulnerability (adaptive capacity) | –  |

socioeconomic dynamics that influence the resilience and vulnerability of coastal cities to climate-related hazards. The integration of these indicators into the MHRA, contextualizing them within the framework of exposure, sensitivity, and adaptive capacity, is aimed at identifying patterns, assessing needs, and informing targeted, context-specific strategies for enhancing urban resilience.

### 2.8. Risk calculation

The methodology for scoring the indicators hinges on the analysis of a diverse array of cases, which are deemed adequate for establishing benchmarks against which the indicators can be evaluated. These benchmarks derive from the extremities of observed values for each indicator, specifically the minimum and maximum recorded values. To facilitate a baseline methodology for the scoring and aggregation of

these indicators, a normalized scoring system is employed, wherein each indicator value for the cities under consideration is assigned a score within the interval  $[0, 1]$ , corresponding to its relative position between the observed extremities, with the exception of critical elements indicators, which were ascribed binary scores of 0 or 1. This normalization process employs the linear scale transformation of min-max method to map the raw indicator values to their respective scores (Hwang and Yoon, 2012).

Denoting  $I_{ij}$  the raw value of the  $i$ -th indicator for the  $j$ -th city, with  $i = 1, 2, \dots, N$  and  $j = 1, 2, \dots, M$ , where  $N$  is the total number of indicators and  $M$  is the total number of cities analysed, the normalization of these values into scores,  $S_{ij}$ , is accomplished as per

$$S_{ij} = \frac{(S_{i,max} - S_{i,min})(I_{ij} - I_{i,min})}{I_{i,max} - I_{i,min}} + S_{i,min}, \quad (1)$$

where  $I_{i,min}$  and  $I_{i,max}$  represent the minimum and maximum values recorded for the  $i$ -th indicator across all cities, and  $S_{i,min}$  and  $S_{i,max}$  are equal to 0 and 1, respectively.

Indicators were systematically classified under the paradigms of hazard, exposure, or vulnerability. A holistic score per category was derived, facilitating an aggregate risk assessment, wherein equal weights were applied, in alignment with recent related studies (Bagdanavičiūtė et al., 2019; Godwyn-Paulson et al., 2022; Hagenlocher et al., 2018; Sahoo and Bhaskaran, 2018; Tiepolo et al., 2019). To compute the composite score for each category  $C_k$  in the  $j$ -th city, the scores of the indicators within each category are aggregated,

$$A_{C_k,j} = \frac{\sum_{i \in C_k} S_{ij}}{N_{C_k}}, \quad (2)$$

where  $N_{C_k}$  denotes the number of indicators within risk category  $C_k$ , namely hazard, exposure and vulnerability. The indicators which has reverse effect on vulnerability, i.e., indicators of adaptive capacity, were subtracted from 1 for consistency.

The components of hazard, exposure and vulnerability were integrated into a final European Multi-hazard Index (*EMI*) score of risk through multiplicative aggregation. For this calculation, the risk components were equally weighted according to

$$EMI_j = \prod_k A_{C_k,j}, \quad (3)$$

where  $EMI_j$  denotes the risk for the  $j$ -th city and  $k$  ranges between the number of components of risk, thus  $k = 1, 2, 3$ . The complete list of indicators and their corresponding notation is provided in Table 4. The results encompass maps and graphs elucidating both individual and aggregated indicators scores. To improve the interpretability of the risk assessment results, the cubic root transformation was applied to the calculated risk values. This transformation helps normalize the data and stabilize variance, making the results more intuitive, especially for extreme values. The cubic root of risk allows for a more balanced representation of low and high-risk areas, facilitating easier comparison and prioritization of risk management actions. The transformed risk values were used in all subsequent analyses and visualizations to ensure consistency and clarity in the interpretation of the findings.

It is noteworthy that despite the representativeness of the values for setting thresholds in Europe, the sample size precludes extensive correlation analyses among variables. This limitation guided the methodological decision to eschew variance-based weighting techniques such as sphericity tests, Kaiser-Meyer-Olkin measure, and principal component analysis (Petzold and Ratter, 2015).

## 3. Results

The main objective of this study is to integrate the diverse indicators of risk in a systematic and standardized approach, enabling a comprehensive understanding of the risks faced by each city and allowing

**Table 4**  
Summary of indicators, including their units, corresponding parameter of risk and label.

| Label | Indicator                                       | Units                       | Parameter of risk                 |
|-------|---|-----------------------------|-----------------------------------|
| H1    | Area susceptible to landslides                  | % of total area             | Hazard                            |
| H2    | Land flooding area                              | % of total area             | Hazard                            |
| H3    | Yearly averaged number of strong wind events    | Year <sup>-1</sup>          | Hazard                            |
| H4    | Yearly averaged number of heavy rainfall events | Year <sup>-1</sup>          | Hazard                            |
| H5    | Extreme high temperature threshold              | °C                          | Hazard                            |
| H6    | Extreme low temperature threshold               | °C                          | Hazard                            |
| H7    | Yearly averaged number of heatwave days         | day/year                    | Hazard                            |
| H8    | Yearly averaged number of cold spell days       | day/year                    | Hazard                            |
| H9    | Yearly averaged number of drought months        | month/year                  | Hazard                            |
| H10   | Mean sea-level rate                             | mm/year                     | Hazard                            |
| H11   | Coastline length undergoing erosion             | % of total coastline length | Hazard                            |
| H12   | Significant wave height                         | m                           | Hazard                            |
| H13   | Surge level                                     | m                           | Hazard                            |
| H14   | Annual highest high tide                        | m                           | Hazard                            |
| E1    | Area  | km <sup>2</sup>             | Exposure                          |
| E2    | Population density                              | inhabitants/km <sup>2</sup> | Exposure                          |
| E3    | Residential area                                | % of total area             | Exposure                          |
| V1    | Open areas                                      | % of total area             | Vulnerability (adaptive capacity) |
| E4    | Critical infrastructure area                    | % of total area             | Exposure                          |
| E5    | Transportation infrastructure area              | % of total area             | Exposure                          |
| E6    | Agriculture area                                | % of total area             | Exposure                          |
| E7    | Forest area                                     | % of total area             | Exposure                          |
| E8    | Wetland area                                    | % of total area             | Exposure                          |
| V2    | Presence of power plant                         | Yes/No                      | Vulnerability (sensitivity)       |
| V3    | Presence of airport                             | Yes/No                      | Vulnerability (sensitivity)       |
| V4    | Presence of port                                | Yes/No                      | Vulnerability (sensitivity)       |
| V5    | Presence of railway                             | Yes/No                      | Vulnerability (sensitivity)       |
| E9    | LECZ area                                       | % of total area             | Exposure                          |
| E10   | Residential area (LECZ)                         | % of LECZ area              | Exposure                          |
| V6    | Open areas (LECZ)                               | % of LECZ area              | Vulnerability (adaptive capacity) |
| E11   | Critical infrastructure area (LECZ)             | % of LECZ area              | Exposure                          |
| E12   | Transportation infrastructure area (LECZ)       | % of LECZ area              | Exposure                          |
| E13   | Agriculture area (LECZ)                         | % of LECZ area              | Exposure                          |
| E14   | Forest area (LECZ)                              | % of LECZ area              | Exposure                          |
| E15   | Wetland area (LECZ)                             | % of LECZ area              | Exposure                          |
| V7    | Presence of power plant (LECZ)                  | Yes/No                      | Vulnerability (sensitivity)       |
| V8    | Presence of airport (LECZ)                      | Yes/No                      | Vulnerability (sensitivity)       |
| V9    | Presence of port (LECZ)                         | Yes/No                      | Vulnerability (sensitivity)       |
| V10   | Presence of railway station (LECZ)              | Yes/No                      | Vulnerability (sensitivity)       |
| V11   | Population over 65 years old                    | % of total population       | Vulnerability (sensitivity)       |
| V12   | Population under 5 years old                    | % of total population       | Vulnerability (sensitivity)       |
| V13   | Unemployment                                    | % of total population       | Vulnerability (sensitivity)       |
| V14   | GDP per capita                                  | % of total population       | Vulnerability (adaptive capacity) |
| V15   | Economically active population                  | % of total population       | Vulnerability (adaptive capacity) |
| V16   | Higher education                                | % of total population       | Vulnerability (adaptive capacity) |

comparisons with other European coastal cities. The hazard indicators consolidate abundant information from diverse climate-related hazards. In this vein, graphical representations are crucial for visualizing and interpreting the spatial and temporal distributions of these hazards. Fig. 3 is an example for Klaipeda, designed to provide insights into the calculation process of the hazard indicators before their normalization, employing GIS and calculation software. The map on the left of the figure highlights the LECZ and coastal erosion trends, where the areas experiencing significant erosion are marked in red. The LECZ area, calculated from MERIT DEM and expressed as a percentage of the total city area for comparison, results in 42.2%, the highest value among the study cases. This significant percentage indicates that nearly half of the area of Klaipeda area is susceptible to sea-level rise and related coastal hazards. Similarly, the length of coastline undergoing erosion, measured from EuroSION data and expressed as a percentage of the total coastline length, yields a relatively low value of 12.7%. This lower percentage suggests that while coastal erosion is present, it affects a smaller portion of the coastline compared to other hazards. The middle map illustrates the extents corresponding to the 100-year river flooding event, as per Dottori et al. (2021), marked in pink, indicating flood-prone areas due to their proximity to the Danė River and low-lying topography. These flood-prone areas are critical for urban planning and infrastructure development, as they highlight zones that may be affected by compound flooding hazard. The map on the right shows the distribution of landslide susceptibility in Klaipeda according to Wilde et al. (2018), categorized as very low, low, medium, high, and very high. The indicator accounts only for areas with high and very high susceptibility levels. In Klaipeda, these levels are not reached, indicating a low landslide hazard. However, the presence of any susceptible areas, even at lower levels, warrants continuous monitoring, especially in zones with significant human activity or infrastructure.

The bar charts below the maps show the yearly distribution of heatwaves, cold spells, heavy rainfall events, and droughts. The extreme temperature thresholds provided, -19.0 °C and 29.0 °C, were employed to calculate the heatwave and cold spell events, defined as periods of at least three days exceeding these thresholds (Lavaysse et al., 2018). Klaipeda experiences approximately 2.0 days of heatwaves per year, while cold spells occur approximately 0.8 days per year. These frequencies summarize the total number of days per year for these events and are crucial for public health planning and energy management, particularly during extreme temperature events. The indicators for heavy rainfall and droughts summarize the yearly average of precipitation events exceeding 20 mm/day and meteorological drought months where SPI-3 is below -1, respectively. Klaipeda experiences about 1.8 days of heavy rainfall per year, whereas droughts occur approximately 2.1 months per year. These rainfall and drought indicators are essential for water resource management and agricultural planning, providing insights into the frequency and severity of these events. The indicators measure the yearly average for these hazards, though the graphs also aid in understanding the temporal evolution and potential trends. For example, an uptrend in heatwaves and a downtrend in droughts can be noted, providing critical insights into the changing climate dynamics in Klaipeda. Understanding these trends is vital for developing adaptive strategies to mitigate the impacts of climate change, ensuring the resilience and sustainability of the city.

The comparative assessment of these indicators reveals distinct patterns that reflect the unique climatic and geographical context of each city. Another example before the normalization of the indicators is illustrated in Fig. 4, covering extreme sea levels and sea-level rise. The data reveal a clear demarcation between cities subjected to the influence of the Atlantic Ocean and those sheltered within the Mediterranean basin. The bar chart on the left illustrates the annual highest high tide, surge level, and significant wave height for the six cities. These indicators provide an estimation of the extreme sea-levels that the cities can potentially suffer from, based on data from ERA5 reanalysis (Caires and Yan, 2020; Hersbach et al., 2020; Yan et al., 2020). The map on the



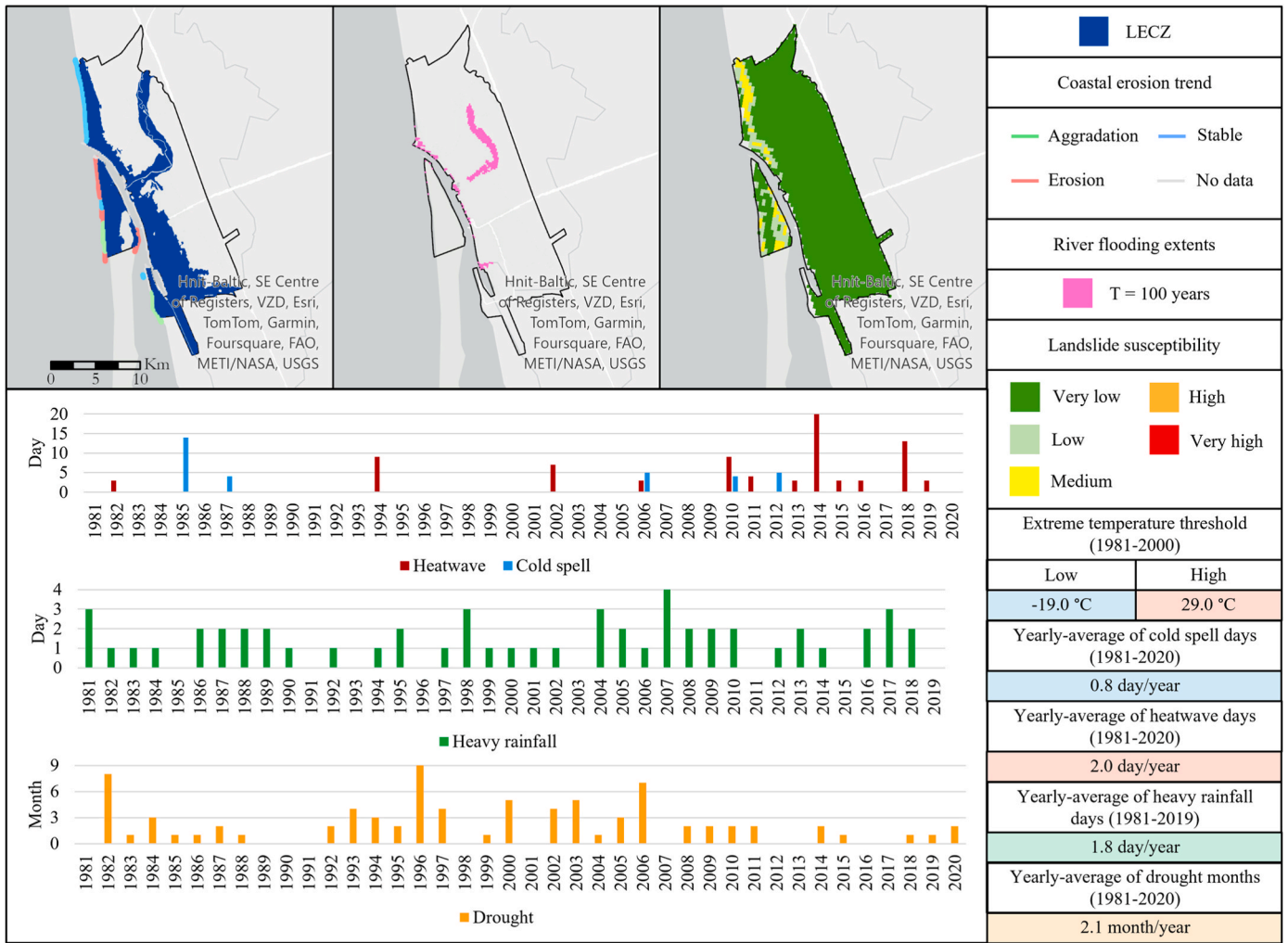


Fig. 3. Graphical visualization of some indicators of hazard for Klaipeda, including LECZ area, coastal erosion trend, river flooding area, landslide susceptibility, extreme temperature thresholds, and heatwave, cold spell, heavy rainfall and drought frequencies. Data source: Dottori et al. (2021), European Commission and Joint Research Centre (JRC) (2021), Lavaysse et al. (2018), Lenôtre et al. (2004), Mercogliano et al. (2021), Wilde et al. (2018) and Yamazaki et al. (2017).

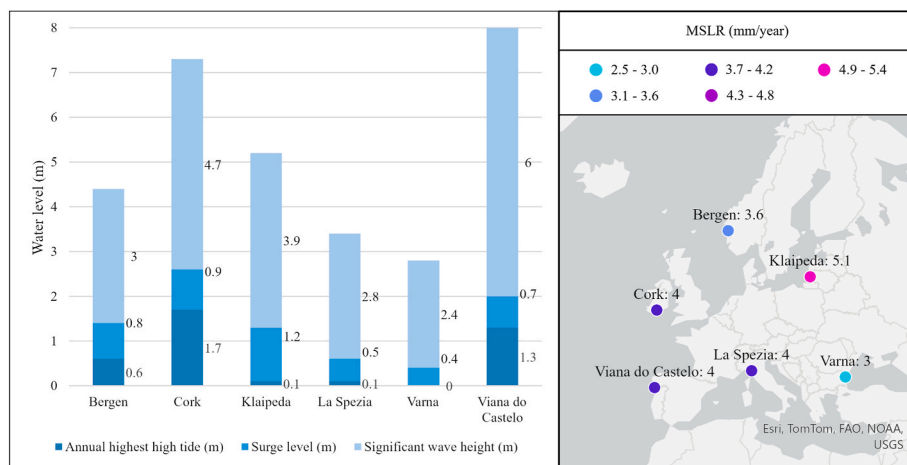


Fig. 4. Indicators regarding sea-level rise and extreme sea-levels. Data source: Caires and Yan (2020), Hersbach et al. (2020), Kopp et al. (2023) and Yan et al. (2020).

right of the figure shows the baseline MSLR rates for these cities, based on data from NASA for the year 2020 under the RCP4.5 scenario (Garner et al., 2021; Kopp et al., 2023), with colour coding representing different

rates of rise ranging between 3.0 mm/year and 5.1 mm/year. The data highlight the varying impacts of sea-level rise and extreme sea levels on the coastal cities. Atlantic cities, particularly Cork and Viana do Castelo,

are subject to higher extreme sea levels compared to Mediterranean cities, likely due to more significant wave heights and storm surges. Viana do Castelo displays the highest combined water level, with an annual highest high tide of 1.3 m, a surge level of 1.4 m, and a significant wave height of 6.0 m, resulting in a total extreme water level of approximately 8.7 m. The MSLR rates also vary, with Klaipeda experiencing the highest rate of sea-level rise, suggesting a need for tailored coastal management and mitigation strategies to address these specific challenges.

The complete set of hazard indicators encompass a spectrum of climate-related phenomena, including extreme weather events and long-term climatic shifts. The heatmap visualization in Fig. 5 synthesizes these observations after min-max normalization, based on the data from Table 5, which summarizes the values obtained for the indicators, offering a comparative view of hazard intensities across the cities. The indicators demonstrate the capacity to discern subtle differences between these urban areas. La Spezia emerges as a focal point for hazard intensity, with near-maximal scores in indicators associated with landslides, extreme temperatures, heatwaves, cold spells, and droughts – a reflection of the vulnerability inherent to the trend towards desertification of the Mediterranean region. In contrast, coastal and riverine flooding hazards, along with strong winds, are comparatively subdued here, likely due to the mitigating effects of the Mediterranean climate. Indicators of sea-level rise and heavy precipitation also display moderate values, suggesting a nuanced hazard landscape. The oceanic climate of Cork is reflected in mild extremes in temperature but heightened indicators for heavy rainfall and strong winds – conditions that are echoed in Viana do Castelo, albeit with a slightly warmer, less volatile climate. These cities exemplify the propensity of Atlantic climate for dynamic weather patterns, characterized by significant precipitation and strong wind events. La Spezia and Varna, with their minimal scores, epitomize the sheltering effects of the Mediterranean Sea and the relative calm of the Black Sea, respectively.

The contrasting hazard profiles of cities influenced by the Atlantic Ocean versus those within the Mediterranean basin have significant implications for urban planning and emergency management. In Atlantic-facing cities like Cork and Viana do Castelo, the focus might be on strengthening coastal defences against storms and enhancing flood-prevention measures. In contrast, Mediterranean cities may prioritize coping with extreme heat and ensuring water security. This understanding may guide city planners in allocating resources and developing tailored risk mitigation strategies. Cities with challenging topographies, notably La Spezia and Bergen, exhibit heightened landslide hazards. The position of La Spezia amongst hills and the topography of Bergen, characterized by mountains and fjords, contribute to their pronounced susceptibility to landslides. Conversely, flatter urban landscapes, particularly evident in Cork, show a predisposition towards river flooding, which highlights the interplay between topography and hazard potential. For cities like Cork, the historical development along riverbanks may contribute to its higher river flooding scores.

The exposure of the coastal cities to the previous climate-related hazards is evaluated by examining land use and population density

metrics in the total area in both the total area of study and the LECZ. These indicators are compared in the heatmap shown in Fig. 6. Regarding the total coverage, Bergen covers the largest area among the cities studied (465 km<sup>2</sup>), suggesting a broad interface with natural environments that may influence exposure patterns. Viana do Castelo also spans a considerable area (319 km<sup>2</sup>), indicative of its reach along the coastline. In contrast, La Spezia and Cork are more compact (51.5 km<sup>2</sup> and 39.6 km<sup>2</sup>, respectively), which emphasizes the diversity in city sizes and the potential concentration of risks in smaller urban spaces.

Klaipeda exhibits an extensive LECZ, covering almost one-half of the total area, which explains its vulnerability to sea-level rise and coastal flooding. Cork, La Spezia, and Viana do Castelo also have notable LECZ areas, albeit less extensive than Klaipeda. Bergen and Varna have the smallest LECZ proportions (2.3% and 5.3%, respectively), suggesting a lower direct exposure to sea-level influences. Historically, the development of Klaipeda has been closely tied to its port, with economic activities concentrated along the coast. The extensive LECZ implies a heightened susceptibility to sea-level rise and coastal storms, which could disrupt these critical economic activities. A deeper exploration into the urban planning and coastal defences could reveal strategies for mitigating this exposure, such as the implementation of green infrastructure or revised zoning laws designed to reduce the concentration of critical assets and populations in vulnerable areas.

High population density is a critical component of exposure, as may be seen in Cork, which could lead to amplified impacts from climate hazards. Varna, La Spezia, and Klaipeda have similar population densities, while Bergen and Viana do Castelo have lower densities, possibly providing more space for dispersion of risks. In Cork, the high population density within a constrained urban area intensifies the potential impact of climate-related events. This density, when overlaid with the LECZ, reveals a compounded vulnerability. Areas of high population density that coincide with high-risk zones may face challenges in emergency response and evacuation efficiency. It is essential that urban planning strategies be developed to incorporate these factors into risk assessments, ensuring that evacuation routes, emergency shelters, and infrastructure are designed to handle the demands of a dense population facing a heightened risk of flooding and other coastal hazards.

The level of urbanization within these cities varies widely. Cork is the most urbanized, with extensive residential and infrastructure development. Bergen and Viana do Castelo show a lower level of urbanization, which is evident in the distribution of land uses (Fig. 7). The size and spread of residential areas influence not just the density of the population but also the capacity of the city to respond to emergencies. More urbanized areas may face greater challenges in mobilizing resources and managing evacuations, especially if the infrastructure is not designed with resilience in mind. The analysis of urbanization should therefore be coupled with an assessment of emergency preparedness, including the adequacy of evacuation routes and the accessibility of safe zones.

When analysing the total area, Cork has a notably larger residential area compared to Bergen, reflecting its urban density. The distribution of residential, infrastructure, and transportation areas varies with the degree of urbanization. Forest and agricultural lands tend to be more prevalent in less urbanized cities. Wetland distribution does not directly correlate with urbanization levels – it may show high values in both urbanized and less urbanized settings. Focusing on the LECZ, the trend shifts. The residential area of Bergen is relatively large within the LECZ – a somewhat counterintuitive finding considering the overall urban profile of the city. Cork shows moderate values, whereas La Spezia has significant critical infrastructure and transport areas within its LECZ. The wetland areas see a substantial increase within the LECZ, which could have implications for biodiversity and ecosystem services in these zones.

Notwithstanding, the role of wetlands, particularly within the LECZ, is multifaceted. In Varna, the increase in wetland areas within the LECZ (from 5.1% to 47.6%) could be seen as a potential asset, providing natural buffers that mitigate exposure to storm surges and flooding. The

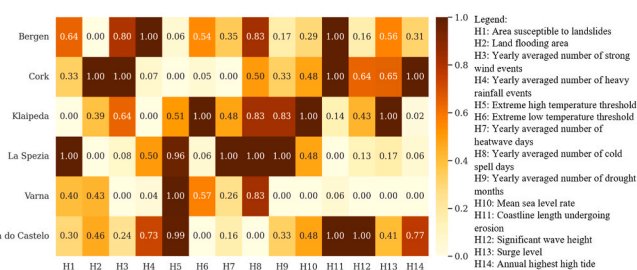
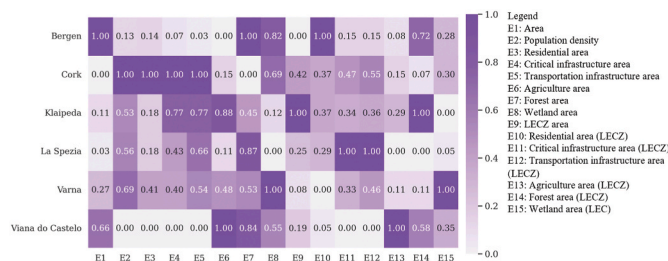


Fig. 5. Heatmap representation of the indicators of hazard after min-max normalization to a range of 0–1.

**Table 5**  
Results of the indicator-based assessment.

| Indicator  | Bergen       | Cork          | Klaipeda      | La Spezia     | Varna         | Viana do Castelo |
|--|--------------|---------------|---------------|---------------|---------------|------------------|
| Landslide-prone area (%)                         | 41.6         | 21.4          | 0.0           | 64.6          | 26.1          | 19.7             |
| Land flooding area (%)                           | 0            | 10.3          | 4.0           | 0             | 4.4           | 4.7              |
| Strong winds frequency (event/year)              | 2.0          | 2.5           | 1.6           | 0.2           | 0.0           | 0.6              |
| Heavy rainfall frequency (day/year)              | 46.9         | 4.8           | 1.8           | 24.5          | 3.8           | 34.6             |
| Extreme high temperature threshold (°C)          | 25.0         | 24.5          | 29.0          | 33.0          | 33.4          | 33.3             |
| Extreme low temperature threshold (°C)           | -11.0        | -2.5          | -19.0         | -2.8          | -11.6         | -1.7             |
| Heatwave frequency (day/year)                    | 1.6          | 0.5           | 2.0           | 3.6           | 1.3           | 1.0              |
| Cold spell frequency (day/year)                  | 0.8          | 0.6           | 0.8           | 0.9           | 0.8           | 0.3              |
| Drought frequency (month/year)                   | 1.7          | 1.8           | 2.1           | 2.2           | 1.6           | 1.8              |
| Mean sea-level rate (mm/year)                    | 3.6          | 4             | 5.1           | 4             | 3             | 4                |
| Coastline length undergoing erosion (%)          | 50           | 50            | 12.7          | 0             | 5.2           | 88.2             |
| Significant wave height (m)                      | 3            | 4.7           | 3.9           | 2.8           | 2.4           | 6                |
| Surge level (m)                                  | 0.8          | 0.9           | 1.2           | 0.5           | 0.4           | 0.7              |
| Annual highest high tide (m)                     | 0.6          | 1.7           | 0.1           | 0.1           | 0             | 1.3              |
| Area (km <sup>2</sup> )                          | 464.7        | 39.6          | 88.2          | 51.5          | 154.0         | 319.0            |
| Population density (inhabitant/km <sup>2</sup> ) | 622.7 (2022) | 2996.6 (2011) | 1725.1 (2022) | 1791.3 (2022) | 2160.3 (2022) | 269.6 (2022)     |
| Residential area (%)                             | 16.0         | 45.2          | 17.2          | 17.4          | 25.0          | 11.1             |
| Open areas (%)                                   | 6.3          | 11.6          | 4.8           | 2.6           | 5.0           | 1.2              |
| Critical infrastructure area (%)                 | 2.5          | 16.5          | 13.1          | 8.0           | 7.5           | 1.5              |
| Transportation infrastructure area (%)           | 3.3          | 11.7          | 9.7           | 8.7           | 7.7           | 3.0              |
| Agriculture area (%)                             | 3.9          | 7.1           | 22.6          | 6.3           | 14.1          | 25.2             |
| Forest area (%)                                  | 63.3         | 1.6           | 29.6          | 55.1          | 34.2          | 53.2             |
| Wetland area (%)                                 | 4.2          | 3.6           | 0.8           | 0.2           | 5.1           | 2.9              |
| Presence of power plant (0 or 1)                 | 1.0          | 0.0           | 1.0           | 0.0           | 0.0           | 1.0              |
| Presence of airport (0 or 1)                     | 1.0          | 0.0           | 0.0           | 0.0           | 1.0           | 0.0              |
| Presence of port (0 or 1)                        | 1.0          | 1.0           | 1.0           | 1.0           | 1.0           | 1.0              |
| Presence of railway station (0 or 1)             | 1.0          | 1.0           | 1.0           | 1.0           | 1.0           | 1.0              |
| LECZ area (%)                                    | 2.3          | 19            | 42.2          | 12.3          | 5.3           | 9.9              |
| Residential area (LECZ) (%)                      | 36.5         | 15.5          | 15.5          | 12.9          | 3.1           | 4.9              |
| Open areas (LECZ) (%)                            | 3.6          | 16.5          | 5.4           | 10            | 5.7           | 4.7              |
| Critical infrastructure area (LECZ) (%)          | 6.8          | 17.7          | 13.1          | 35.5          | 12.6          | 1.6              |
| Transportation infrastructure area (LECZ) (%)    | 8.8          | 20.8          | 15.1          | 34.7          | 18.2          | 4.1              |
| Agriculture area (LECZ) (%)                      | 3.8          | 6.7           | 11.9          | 0.7           | 5.1           | 39.7             |
| Forest area (LECZ) (%)                           | 25.4         | 3.1           | 34.9          | 0.7           | 4.3           | 20.5             |
| Wetland area (LECZ) (%)                          | 14.7         | 15.6          | 1.8           | 3.8           | 47.6          | 18               |
| Presence of power plant (LECZ) (0 or 1)          | 0            | 0             | 0             | 0             | 0             | 1                |
| Presence of airport (LECZ) (0 or 1)              | 1            | 0             | 0             | 0             | 0             | 0                |
| Presence of port (LECZ) (0 or 1)                 | 1            | 1             | 1             | 1             | 1             | 1                |
| Presence of railway station (LECZ) (0 or 1)      | 1            | 1             | 0             | 1             | 1             | 0                |
| Population over 65 years old (%)                 | 14.5 (2013)  | 15 (2011)     | 19.5 (2018)   | 26.7 (2018)   | 17.5 (2018)   | 22.4 (2019)      |
| Population under 5 years old (%)                 | 6.4 (2011)   | 5.1 (2011)    | 5.2 (2022)    | 3.6 (2022)    | 4.8 (2022)    | 3.7 (2022)       |
| Unemployment (%)                                 | 0.9 (2011)   | 8.9 (2011)    | 3.3 (2022)    | 4.8 (2020)    | 3 (2021)      | 2.8 (2021)       |
| GDP per capita                                   | 50,300       | 144,000       | 16,600        | 29,800        | 8000          | 15,700           |
| Economically active population (%)               | 25.8 (2021)  | 45.2 (2011)   | 54.8 (2022)   | 44.6 (2020)   | 46.8 (2021)   | 45.8 (2021)      |
| Higher education (%)                             | 14.4 (2022)  | 16.3 (2011)   | 27.5 (2022)   | 11.4 (2021)   | 25.9 (2022)   | 13.7 (2022)      |



**Fig. 6.** Heatmap representation of the indicators of exposure after min-max normalization to a range of 0–1.

conservation and restoration of wetlands should be integral to climate adaptation strategies, leveraging these ecosystems to provide natural defences that complement engineered solutions. This balance between the natural and built environments can be crucial for building a resilient urban landscape.

It is important to note that the use of administrative boundaries to define the study areas can influence the exposure indicators and, therefore, risk. To address this, alternative methods could be employed, such as delineating study areas based on physical geography, such as watersheds or topographical features, or using population density maps

to identify areas of high human concentration. These approaches would provide different perspectives on the spatial dynamics of hazard exposure and vulnerability. Additionally, incorporating participatory GIS methods could engage local communities in identifying and validating high-risk zones, leading to a more nuanced and grounded understanding of exposure.

LULC patterns extend beyond exposure to encapsulate sensitivity, crucial for understanding the nuanced responses of coastal cities to climate-related hazards. For example, urban areas, characterized by their impervious surfaces, directly influence water runoff and drainage dynamics, intensifying flood risks. As previously discussed, Cork exhibits higher urbanization rates when considering the total study area, yet within their respective LECZs, both Cork and Bergen share a similar percentage of urbanized land (52.1% and 54.0%, respectively, when residential, critical infrastructure, and transportation are accounted for). This parity indicates a substantial presence of sensitive and impervious areas within the LECZ of Bergen, raising its vulnerability to coastal hazards. A similar trend is observed in La Spezia, indicating an increased sensitivity within these regions.

Urbanized regions also contribute to the Urban Heat Island (UHI) effect, where temperatures in built-up areas exceed those of surrounding rural regions. This phenomenon can amplify the effects of heatwaves, with repercussions for public health and energy demand. La Spezia, with

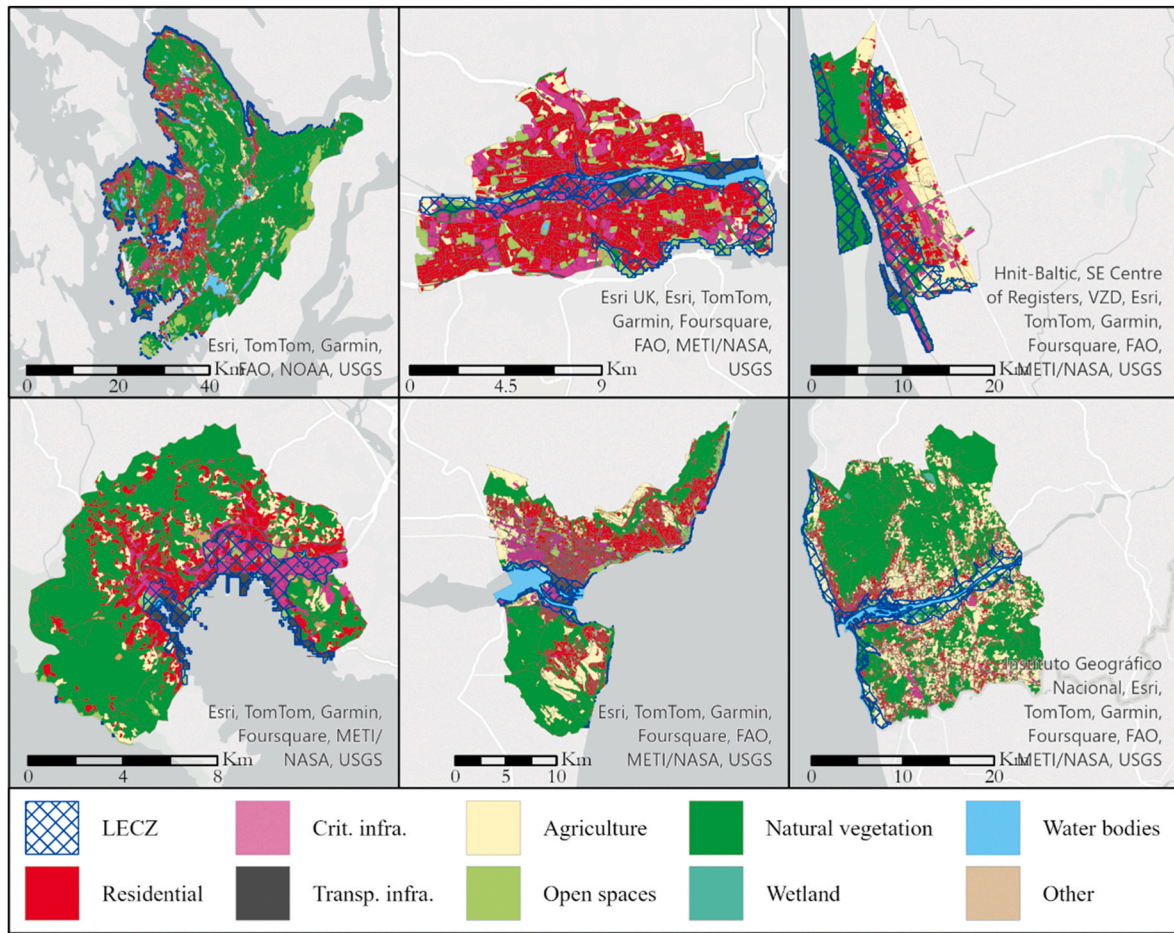


Fig. 7. Map of land uses based on the reclassification of Urban Atlas categories and low-elevation coastal zones.

its significant urban areas and high heat hazard and drought indicators, must prioritize addressing these risks. Planning should incorporate green spaces and reflective materials in urban design to mitigate the UHI effect. Furthermore, LULC is intricately linked to socioeconomic dynamics. Land uses such as forests and wetlands may display less sensitivity to flooding but are more vulnerable to temperature and precipitation hazards. Conversely, agricultural lands may be sensitive to a wider array of dangers. This intricate relationship is reflected in the indicators for Viana do Castelo.

The spatial distribution of infrastructure and essential services critically shapes the vulnerability profile of cities (Fig. 8). Ensuring that infrastructure such as hospitals, power plants, and water treatment facilities is not only robust but also strategically sited is paramount. Data from OpenStreetMap reveal commonalities across the cities, with ports

being a universal feature within the LECZ. Notably, Klaipeda and Viana do Castelo lack railway stations within their LECZs. Only Bergen and Viana do Castelo have airports within the study area, with the airport of Bergen also falling within the LECZ. Power plants are present only on the periphery of Bergen, Klaipeda, and Viana do Castelo, with the facility of Viana do Castelo located within the LECZ, potentially increasing its sensitivity to coastal hazards.

Demographic profiles, especially the proportion of vulnerable age groups (under 5 and over 65), are indicative of sensitivity. These groups typically require additional resources during climate events due to their specific needs and lower resilience. Fig. 9 illustrates the evolution of these indicators, including the rates of unemployment and economically active population, based on data from Eurostat. Most recent data show that La Spezia has the oldest population (26.7%), followed by Viana do

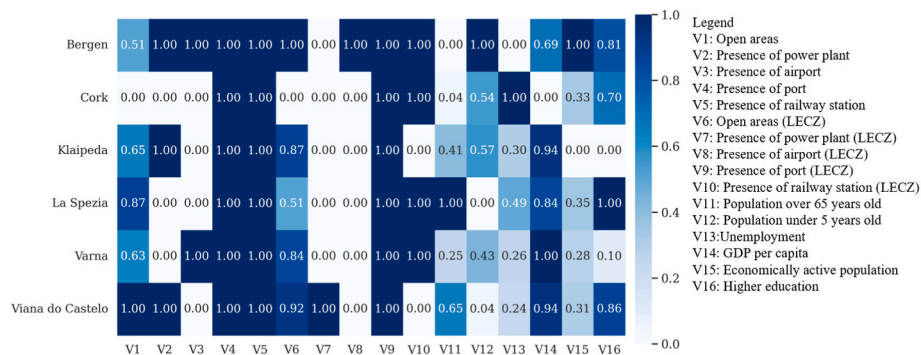


Fig. 8. Heatmap representation of the indicators of vulnerability after min-max normalization to a range of 0–1.

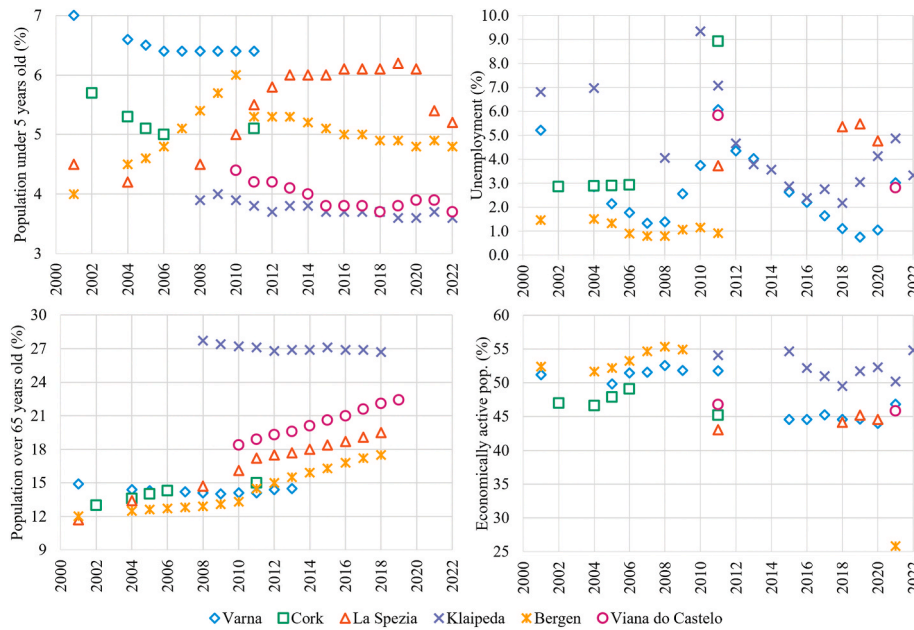


Fig. 9. Evolution of indicators on population. Data source: Eurostat.

Castelo (22.4%) and Klaipeda (19.5%), while Bergen and Cork are at the lower end (14.5% and 15.0%, respectively). The youngest populations are found in Bergen (6.4%), Cork, and Klaipeda (5.1% and 5.2%), contrasting with La Spezia (3.6%) and Viana do Castelo (3.7%), characterized by aging demographics.

Unemployment rates serve as an indirect indicator of the economic resilience to climate-related shocks. For Bergen, the unemployment rate was last recorded at 0.9% in 2011. In contrast, Cork had an unemployment rate at the time of 8.9%. Notably, the unemployment rate in Bergen, although based on older data, is the lowest among the cities studied, occasionally matched only by Varna during brief periods. The most recent rates of unemployment available for the other cities are 3.3% for Klaipeda (in 2022), 4.8% for La Spezia (in 2020), 3.0% for Varna (in 2021), and 2.8% for Viana do Castelo (in 2021). While historical data for some cities show lower unemployment rates, the 2020–2022 figures provide a more contemporaneous assessment for these urban areas. It is important to note that data for Viana do Castelo are quite limited, with only two records available (for 2011 and 2021).

The proportion of economically active population is indicative of economic vibrancy and resilience. This demographic is central in maintaining workforce stability and can indicate how a city might cope with climate-induced economic fluctuations. The data call for careful interpretation, particularly in light of recent disruptions such as the COVID-19 pandemic. Notably, Bergen reported an economically active population of 25.8% in 2021, with an unemployment rate last recorded in 2011. This points to the potential for outdated data to skew the risk assessment. Conversely, Cork’s 2011 figure of 45.2% for the economically active population may no longer reflect current conditions. Recent figures for other cities present a more current assessment, with Klaipeda ranking highest at 54.8% in 2022, La Spezia at 44.6% in 2020, Varna at 46.8% in 2021, and Viana do Castelo at 45.8% in 2021.

GDP per capita serves as a proxy for the availability of resources crucial for climate adaptation and mitigation. A higher GDP per capita suggests a greater potential for investment in resilience-building initiatives. The stark contrast between Cork, with the highest GDP per capita at €144,000, and the rest of the cities, with Bergen at €50,300 and Varna at the lower end with €8,000, underscores the disparity in resource availability for tackling climate challenges.

Higher education correlates with increased awareness and the implementation of innovative strategies to address climate-related

issues. The variability in the level of educational attainment (measured as the percentage of the population over 25 with higher education degrees) between the cities studied is notable, ranging from 27.5% in Klaipeda and 25.9% in Varna to a lower 11.4% in La Spezia and 13.7% in Viana do Castelo. This diversity highlights the importance of education in cultivating adaptive capacity and points to potential areas for investment in human capital.

These results exemplify that risk is not static; it fluctuates significantly over time. The indicators underscore the necessity for a dynamic analysis, calling for continuous monitoring and updating of data to inform adaptive strategies. Only through such rigorous, dynamic evaluation can coastal cities effectively bolster their resilience.

The adaptive capacity has been assessed as a multifaceted concept that hinges on various indicators, including land use patterns, socio-economic dynamics, and educational attainment. Open spaces play a critical role in enhancing the adaptive capacity, for they serve as natural retention areas during flood events, mitigate the urban heat island effect, and can act as firebreaks. Moreover, they improve the overall quality of life, signifying a resilient urban environment. A robust transportation network is equally essential, particularly when mobilizing resources and individuals in response to extreme climate events. Cork stands out in this respect, showcasing a significant proportion of such land uses within both its total study area and the LECZ – particularly regarding open spaces. The LECZ of La Spezia has an extensive transport network, whereas Cork, Klaipeda, and Varna also present noteworthy figures.

The aggregate scores of the indicators are visually represented in Fig. 10 in a scale between 0 and 100. The risk component of hazard exhibits similar scores, between 46 and 50%, for all cities except Varna, which has a score of 25.7 points. However, interpreting this risk score requires nuance when considering individual cities. In Cork and Viana do Castelo, coastal hazards contribute significantly, while land hazards score low. Klaipeda and Bergen show medium scores for both types of hazards. Conversely, La Spezia has very low coastal hazard scores and high land hazard scores, while Varna scores low for both. This analysis highlights the importance of examining individual indicator scores to accurately understand the final risk components.

The exposure component displays medium and low values, ranging from a maximum of 48.6 points in Klaipeda to a minimum of 27.2 points in Viana do Castelo. While detailed analysis of individual indicators

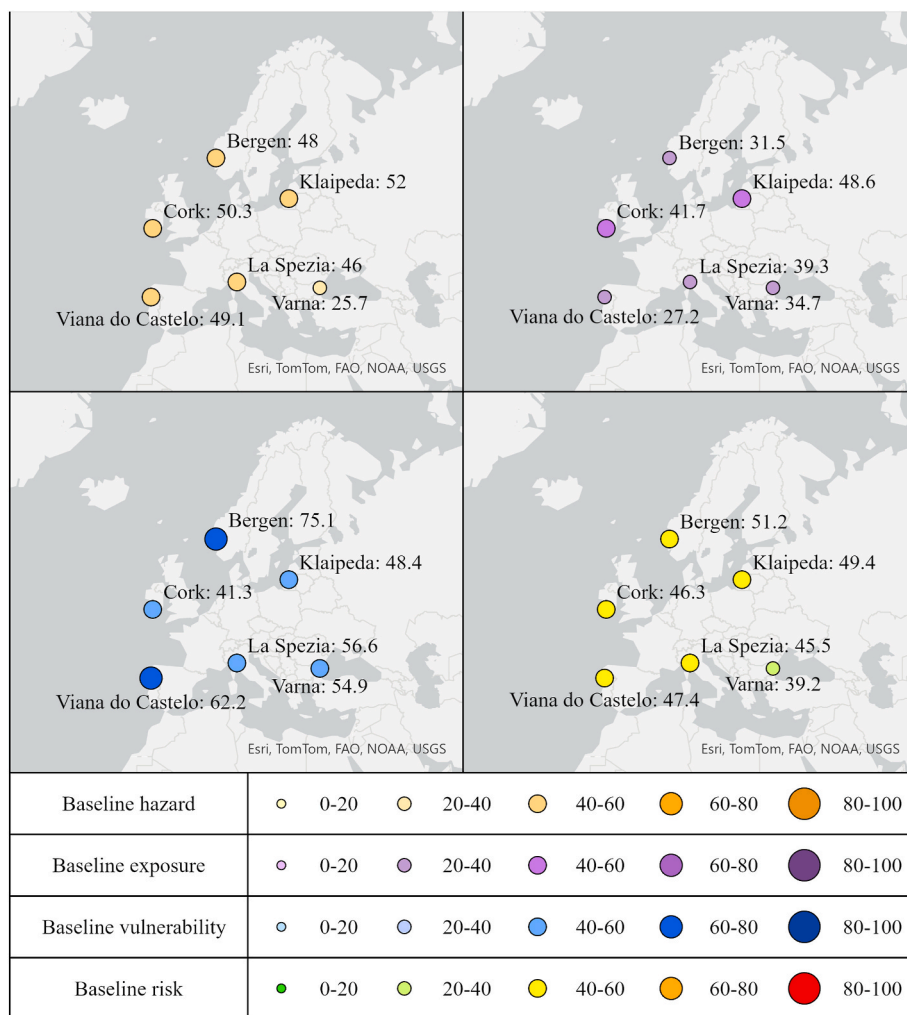


Fig. 10. Results of the indicator-based assessment after the aggregation of the indicators into the risk categories of hazard, exposure, sensitivity and adaptive capacity.

reveals significant differences between cities, such as population density and urbanization levels, the aggregate score masks these variations. The situation is different with regard to vulnerability, where significant variation is found between cities. Viana do Castelo and Bergen stand out for their high scores (62.2 and 75.1 points, respectively) based on the measured indicators. In contrast, Cork exhibits the lowest score (41.3 points). The remaining cities display medium scores, approximately between 45 and 55 points. The substantial annual fluctuations observed in socioeconomic indicators necessitate cautious interpretation of the vulnerability score – it is far from static and depends heavily on the timing of the assessment. Importantly, the vulnerability parameter of adaptive capacity relies on the fewest indicators, which amplifies the relative importance of each individual indicator for the final score.

The observed risk landscape presents a balanced picture, with no city standing out remarkably compared to the others. Interestingly, the cities with the highest scores in hazard and exposure (Cork and Klaipeda) also exhibit the lowest levels of vulnerability. Conversely, Viana do Castelo and Bergen, with lower scores in the initial components, have high vulnerabilities.

#### 4. Discussion

The advancement in risk assessment methodologies for European coastal cities highlighted by this research signifies a notable shift toward methodologies that are not only more inclusive and nuanced but also

dynamic in nature. This shift is paramount in the context of climate change, where the static and compartmentalized approaches of the past are increasingly insufficient to address the complex, interwoven challenges that cities face today. By integrating a broad spectrum of indicators covering hazard, exposure, sensitivity, and adaptive capacity, the methodology introduced herein offers a comprehensive lens through which to view and assess the multifaceted nature of climate risks. Such an approach is invaluable in an era where the impacts of climate change are both far-reaching and deeply interconnected, affecting not just the physical but also the socio-economic fabric of urban areas.

The methodology distinctly advances beyond the scopes of established models like CLIMADA and DIVA, which, while pioneering in their respective foci on natural disaster impacts and sea-level rise, offer a somewhat limited view of climate risk. By broadening the analytical lens to include a wider array of hazards and, crucially, their socio-economic repercussions, the present study addresses a critical gap in the existing literature. It acknowledges that the threats posed by climate change are not isolated incidents but are systemic, with far-reaching implications that necessitate a holistic assessment approach (Sekovski et al., 2020). This is especially pertinent in urban areas, where the density of population and infrastructure magnifies the potential impact of climate hazards (Rangel-Buitrago et al., 2020; Stepanova and Bruckmeier, 2013). Adaptation proposals can thus consider combined hazards, e.g., flooding and landslide, including early warning systems, the prevention of construction in hazard-prone areas, controlled land management

practices, incorporation of green buffers, and implementing sustainable urban drainage systems to mitigate both risks. Notwithstanding, the study acknowledges limitations, such as the inherent uncertainty associated with the selected indicators, the impact of weighting on risk scores, and the potential for representative points to miss intra-city variations in risk. These limitations suggest areas for improvement in future research, highlighting the need for the development of more sophisticated models that account for the spatial heterogeneity of risk within cities and the exploration of alternative weighting schemes to refine risk scoring (Barzehkar et al., 2021).

The comparison of the results with existing studies yields valuable insights. The geographical configuration of Liguria makes it particularly prone to flash floods, storms, forest fires, and landslides (De Angeli et al., 2018; Di Napoli et al., 2021; Sacchini et al., 2012). This is consistent with our findings, where the hazard indicators for La Spezia prominently feature landslides, extreme temperatures, and droughts. Although the indicator for land flooding is negligible, the heavy rainfall indicator is relatively high, especially for a Mediterranean city. This demonstrates the necessity of careful interpretation of indicators, as they may not always provide a clear picture.

In Cork, various studies emphasize the significance of coastal hazards and land flooding, which align well with the indicators (Devoy, 2009; Leahy and Kiely, 2011). The potential compounding of these hazards is a crucial consideration (Moradian et al., 2024). The articles on adaptation and resilience provide guidelines that could be beneficial for other cities that have not advanced as much in these areas (Jeffers, 2011, 2014). This highlights the advantage of comparing cities and sharing results and experiences.

Although the indicators are not very high for Bergen, the study by Venvik et al. (2019) indicates that subsidence is a serious problem in certain areas of the city centre. It also points out that increased precipitation, sea-level rise, and storm surges due to climate change will lead to higher flooding events. The possible combinations of hazards and risks are numerous, and detailed studies are essential to understand the local conditions of each city.

The indicators related to coastal hazards are high in Klaipeda compared to the other cities in this study. However, the application of a coastal risk index along the Baltic Sea shores of Lithuania reveals that the coastal risks in Klaipeda are relatively lower compared to other areas along this coastal strip (Bagdanavičiūtė et al., 2019). This underscores the need for further case studies to broaden our understanding.

In Varna, the hazard indicators highlight extreme temperature hazards more than in other cities, while coastal hazards are relatively low. Nonetheless, the existing literature focuses on coastal hazards, and no studies on extreme temperatures were found (Stanchev et al., 2009; Valchev et al., 2018). This may indicate an underestimation of extreme temperature hazards or an overestimation of coastal hazards in this city. It also underscores the tendency to prioritize coastal hazards in coastal cities over other types of hazards. A more detailed study on the potential impact of extreme temperature hazards and coastal hazards could be illuminating to further explore this disparity.

Southern Europe is generally warmer compared to the rest of Europe. However, Viana do Castelo, located in the northern Iberian Peninsula and exposed to the Atlantic, has an oceanic climate. The indicator results show that the high temperature threshold is significant in this city, along with numerous indicators related to coastal and land flooding, aligning with previous studies (Antunes et al., 2019; Espinosa et al., 2022; Espinosa and Portela, 2022; Grosso et al., 2015; Martins et al., 2012). The drought indicator is low, which aligns with the findings of Santos et al. (2010) indicating that droughts in northwest Portugal are less severe than in the south. The results for Viana do Castelo also prompt reflection on the size of the study area. The study area was defined based on administrative boundaries, which includes large portions of non-urbanized territory, significantly influencing land cover and socio-economic variables.

The adaptability of this methodology is one of its core strengths,

resonating with the latest recommendations from the Intergovernmental Panel on Climate Change for dynamic and comprehensive climate risk frameworks (IPCC, 2014). The ability to incorporate evolving data sets and adapt to the progressing nature of climate science underscores the potential of the methodology for future enhancements and longevity. For example, datasets such as Urban Atlas (of 2018) and Coastal Zones (of 2012 and 2018) from Copernicus were not validated for external use at the moment of writing. Such flexibility ensures that, as the understanding of climate science advances and as new data become available, the methodology can be updated and refined to remain at the forefront of climate resilience planning.

From a theoretical standpoint, this research embodies a shift towards conceptualizing urban resilience within the contexts of adaptability and systemic vulnerability. It aligns with the perspective advocated by Cutter et al. (2003), among others, that resilience transcends mere physical robustness to encompass the adaptive capabilities of urban systems. This approach is crucial for recognizing cities as complex socio-ecological systems, where resilience is contingent upon a multi-faceted strategy that includes not just infrastructural but also social, economic, and environmental considerations (Birkmann et al., 2006). Such a strategy acknowledges the interconnectedness of urban systems and the importance of addressing resilience at multiple scales and dimensions (Frazier et al., 2013). However, while this study provides a comprehensive set of indicators, it acknowledges that the indicators of adaptive capacity are fewer than those for other risk parameters. This discrepancy highlights a limitation of the study, underscoring the challenges in developing adaptive capacity indicators for such assessments.

Notwithstanding, the findings of this study underscore the critical importance of socio-economic factors and community engagement in building adaptive capacity (Berrang-Ford et al., 2021; Holand et al., 2011). In this context, the LULC indicators primarily serve as proxies for exposure to the climate-related hazards. However, the character of these indicators can vary. For example, the presence of green spaces such as parks and urban forests has been recognized for their role in mitigating the impacts of urban flooding by facilitating water infiltration and providing water retention areas, thereby reducing surface runoff and potential flood damage (Aerts et al., 2014a; Flood and Schechtman, 2014; Pelling, 2010). In addition to their hydrological benefits, these green areas offer shade and reduce the urban heat island effect, enhancing urban resilience to heatwaves (Paranunzio et al., 2021; Spalding et al., 2014). Furthermore, strategic placement of urban green spaces can create natural firebreaks that help contain wildfires and protect urban infrastructure (Mitsopoulos and Mallinis, 2017). Transportation infrastructure can also be considered as an element of sensitivity, as any disruption can have cascading effects on the productivity and economic stability of cities (Zahmatkesh and Karamouz, 2017). On the other hand, well-designed transportation networks are integral to emergency response and evacuation processes, enhancing the resilience of cities to disasters (Murray et al., 2021). For instance, the comprehensive allocation of land to open spaces and transport infrastructures underscores a proactive stance in urban planning in Cork (Flood and Schechtman, 2014). However, the dynamic nature of urban development, especially in the aftermath of global disruptions such as the COVID-19 pandemic, necessitates the use of the most current data to accurately gauge these indicators (Kleinschroth et al., 2024). The pandemic has underscored the volatility of urban systems and the critical need for timely data to inform adaptive strategies. Historical data alone may not capture the socio-economic shifts or infrastructural developments that impact resilience capacity in real time.

The literature on adaptive capacity emphasizes the importance of economic activity and workforce stability as resilience metrics (Adger et al., 2003). The data presented suggest that cities like Klaipeda and Varna have vibrant economic profiles, potentially translating into greater adaptive capacities. Yet, the aforementioned limitation of data currency remains pertinent, signalling the need for ongoing data

collection and interpretation. While GDP per capita is a traditional marker of resource availability for climate adaptation, it offers a narrow lens on the overall adaptive capacity of a city. The adaptive capacity is also significantly influenced by its public health infrastructure, which dictates the ability to respond to, and recover from, health-related climate impacts. Social equity and community engagement levels are additional dimensions that determine how inclusive and comprehensive adaptive measures are (Maloutas, 2024). These factors warrant incorporation into the adaptive capacity assessment, for the purpose of providing a more holistic understanding of urban resilience. The educational attainment of the population of a city is a pivotal determinant of its adaptive capacity, equipping residents with the knowledge and skills to implement and support resilience strategies. The variability of the results reflects differential capacities for innovation and adaptation, in line with previous findings (Pelling, 2010) to the effect that education fosters socio-ecological resilience by enhancing the ability of communities to engage with, and adapt to, changing climatic conditions.

This emphasis is also in line with the broader resilience discourse, which highlights the significance of social capital, governance, and institutional flexibility (Adger et al., 2009). These elements are indispensable in equipping cities to navigate and recover from the shocks and stresses related to climate change. The integration of socio-economic indicators into the risk assessment framework not only enriches the analysis but also ensures that the resultant strategies for enhancing resilience are grounded in the realities of urban life (Thomas et al., 2021). It acknowledges that the strength of the response of a city to climate challenges is deeply influenced by the engagement and empowerment of its communities, alongside the robustness of its governance and institutional structures (Blythe et al., 2020).

The policy implications of this research are both significant and timely. The granularity and specificity inherent to the proposed methodology offer a blueprint for urban planners and decision-makers to identify high-risk areas, allowing for a more informed and targeted approach to resilience building. This specificity is particularly crucial in the context of climate adaptation, where the strategic allocation of often limited resources can markedly influence the efficacy of mitigation efforts (Lehmann et al., 2021; Losada et al., 2019). By prioritizing adaptation measures based on a detailed understanding of risk, cities can optimize their resilience strategies, ensuring that investments are directed where they are most needed and can have the greatest impact.

The emphasis on cross-sectoral collaboration and stakeholder engagement as highlighted by this research underscores a critical shift in the paradigm of climate adaptation planning. The integration of diverse perspectives, from local communities to various sectors of governance and industry, is fundamental to the development of robust resilience strategies (Fitton et al., 2021; Petrosillo et al., 2006). This collaborative approach not only enriches the planning process with a multitude of insights and expertise but also ensures that resilience measures are deeply rooted in the local context and are responsive to the specific needs and vulnerabilities of communities (Ashrafal Islam et al., 2016). It highlights the importance of moving beyond top-down approaches to embrace more participatory, inclusive methods of resilience planning, where stakeholders are actively involved in shaping the strategies that affect their lives and environments.

The integration of emerging technologies and innovative methodologies into the framework presents a frontier for enhancing climate risk assessment and adaptation planning (B et al., 2023). The advent of geospatial analytics, artificial intelligence, and citizen science opens up new possibilities for both refining the precision of risk assessments and fostering community engagement in resilience efforts (Barzehkar et al., 2021; Moradian et al., 2023; Riaz et al., 2023). For example, machine learning algorithms applied to vast datasets of climate information could significantly improve the predictability of hazard events, enabling cities to anticipate and prepare for potential impacts with greater accuracy (Assem et al., 2017; de Burgh-Day and Leeuwenburg, 2023; Rodriguez-Delgado et al., 2019). Similarly, participatory GIS and citizen

science initiatives can empower local communities, giving them a voice and stake in identifying vulnerabilities and co-creating solutions, thereby democratizing the process of resilience building (Debaine and Robin, 2012; Kumar et al., 2019; Tiwari et al., 2022).

The exploration of non-traditional indicators, such as digital connectivity, green roofs, psychological resilience, and cultural assets, introduces an innovative dimension to understanding and enhancing urban adaptive capacity (Chen et al., 2018; McClatchey et al., 2014; Nguyen et al., 2016; Vesselinov et al., 2021). These factors, often marginalized in conventional risk assessments, have the potential to unlock new avenues for building resilience (Argyroudis et al., 2022). Recognizing the role of digital infrastructure in facilitating communication and access to information during crises, the importance of mental health and community cohesion in recovery processes, and the value of cultural heritage in fostering a sense of identity and belonging, can all contribute to more resilient urban environments (Chang et al., 2021; Lima and Bonetti, 2020). These dimensions add depth to the understanding of what makes cities resilient, pointing to the need for adaptive strategies that are not only physically robust but also socially and culturally resilient.

This work analyses risk under current climatic conditions. However, considering future scenarios is crucial in climate risk assessment and coastal management (Kirezci et al., 2020; Voudoukas et al., 2018, 2020). Most hazard indicators are based on climate data that can be updated with climate projections, such as sea-level rise, temperature, precipitation, and oceanic variables. Projecting other indicators, specifically coastal erosion, river flooding areas, and landslide susceptibility, poses a greater challenge, though not insurmountable. Data from Urban Atlas, OSM and Eurostat were used for the assessment of the baseline risk. The methodology developed has the potential to be transferable to projecting future risk, which is a crucial step considering the exacerbation of climate-related hazards under climate change. In this respect it is worth mentioning that there are various studies on the urban and demographic evolution of coastal cities throughout this century (Jones and O'Neill, 2016; Merkens et al., 2016; Neumann et al., 2015).

Recent studies show how climate projections might affect the findings of this study until 2100 (Abadie, 2017; Forzieri et al., 2017; Kovats et al., 2014; Voudoukas et al., 2017). According to the latest climate models, global temperatures are projected to rise significantly, likely resulting in more frequent and severe heatwaves in Europe. This increase in temperature could exacerbate heatwave indicator scores for cities already experiencing high temperatures, such as Mediterranean cities, while also impacting cold spell frequencies. Similarly, the desertification of southern Europe poses challenges regarding drought and water availability. Future flooding patterns are also expected to change, with projections indicating increased intensity and frequency of both river and coastal floods. This is particularly relevant for cities like Bergen and Viana do Castelo, which already exhibit high vulnerability to such events. The projected sea-level rise, estimated to reach up to 1 m or more by 2100, will further compound these risks, leading to more extensive coastal erosion.

These changes underline the necessity for proactive urban planning and the integration of adaptive measures to mitigate these impacts. The implications for sustainable coastal management are profound. Integrating climate projections into urban planning is crucial for developing resilient infrastructure and reducing vulnerability (Aerts et al., 2014b; Elmqvist et al., 2019; Laurien et al., 2022). Future recommendations based on these projections include continuous monitoring and updating of climate data and risk assessments. In this sense, the framework applied in this study can be further adapted to other coastal cities by considering local data and conditions. Encouraging collaboration between cities to share best practices and resilience strategies will enhance overall urban resilience. This adaptability is key to accurately assessing and addressing climate risks in diverse geographical contexts. By tailoring the framework to local realities, cities can develop more



effective risk management and adaptation strategies. Adaptive strategies, such as the implementation of green infrastructure, enhanced drainage systems, and robust coastal defences, are vital for managing the anticipated changes. Additionally, increased investment in resilient infrastructure and community engagement in climate adaptation and coastal management initiatives is essential for preparing cities to face future climate challenges.

## 5. Conclusions

By integrating a broad array of indicators covering hazard, exposure, sensitivity, and adaptive capacity, the study provides a novel methodology to assess a wide variety of climate-related risks in European coastal cities. This approach is crucial for addressing the systemic and interconnected impacts of climate change on coastal urban areas, emphasizing the importance of dynamic and comprehensive assessment frameworks. Indeed, the applicability and effectiveness of the proposed methodology are further underscored by its implementation across six diverse European coastal cities: Bergen, Cork, Klaipeda, La Spezia, Varna, and Viana do Castelo. This selection encompasses cities with different climate zones, levels of urbanization, economic profiles, and susceptibility to various climate-related hazards. The findings are consistent with a broad range of existing research, yet our study introduces a novel aspect by enabling comparisons between cities. This approach highlights certain hazards that may not have been extensively studied in some areas but could be significant, underscoring the importance of cross-regional analyses to uncover overlooked risks.

By examining these cities, the research not only validates the comprehensive and dynamic nature of the methodology, but also highlights the importance of contextual factors in climate risk assessment and coastal management. For instance, the distinct climatic influences of the Atlantic Ocean versus the Mediterranean Sea on the selected cities underscore the necessity for location-specific adaptation strategies. Similarly, the study of socioeconomic indicators, such as population density and GDP per capita, across these varied urban contexts reveals how economic and demographic factors significantly influence the adaptive capacity of cities.

The findings highlight the critical role of socio-economic factors, urban planning, and infrastructural resilience in determining the vulnerability and adaptive capacity of coastal cities to climate-related hazards. Urban green spaces, efficient transportation networks, and the spatial distribution of critical infrastructure are identified as key elements that influence the resilience to climate impacts of cities. These factors underscore the necessity of incorporating socio-economic dynamics and community engagement into resilience-building efforts.

The study acknowledges the dynamic nature of climate risk and the importance of continuously updating data and strategies to reflect current conditions. The variability in socio-economic indicators, such as unemployment rates and educational attainment, points to the need for a real-time understanding of urban resilience. This calls for adaptive planning that can respond to evolving climate science and urban development trends.

The granular risk assessment provided by the methodology offers valuable insights for urban planners and policymakers, enabling the identification of high-risk areas and the optimization of coastal management and adaptation strategies. The emphasis on cross-sectoral collaboration and the integration of diverse stakeholder perspectives highlight the shift towards more participatory and inclusive approaches to climate adaptation planning.

The exploration of emerging technologies, such as geospatial analytics and artificial intelligence, presents opportunities for refining risk assessments and enhancing community engagement in resilience efforts. Additionally, considering non-traditional indicators, such as digital connectivity and cultural assets, could provide new dimensions to understanding and enhancing urban adaptive capacity.

In conclusion, the research underscores the complexity of assessing

and addressing climate risks in European coastal cities. It advocates for a multi-dimensional approach that incorporates physical, socio-economic, and infrastructural factors into resilience planning. The dynamic nature of climate change necessitates continuous adaptation and innovation in methodologies and strategies. Engaging a wide range of stakeholders and leveraging emerging technologies are crucial steps towards building resilient urban environments that can withstand the challenges posed by climate change.

## CRedit authorship contribution statement

**Emilio Laino:** Writing – original draft, Visualization, Methodology, Investigation, Formal analysis, Data curation, Conceptualization. **Gregorio Iglesias:** Writing – review & editing, Supervision, Resources, Project administration, Methodology, Conceptualization.

## Declaration of competing interest

The authors declare that they have no known competing financial interests or personal relationships that could have appeared to influence the work reported in this paper.

## Data availability

The authors do not have permission to share data.

## Acknowledgements

The authors acknowledge the support of the European Commission through the SCORE project, SMART CONTROL OF THE CLIMATE RESILIENCE IN EUROPEAN COASTAL CITIES, H2020-LC-CLA-13-2020, Project ID: 101003534. The authors are grateful to the SCORE consortium and, in particular, the Coastal City Living Labs for the valuable local knowledge.

We acknowledge the E-OBS dataset from the EU-FP6 project UERRA (<https://www.uerra.eu>) and the Copernicus Climate Change Service, and the data providers in the ECA&D project (<https://www.ecad.eu>).

Caires and Yan (2020), Hooyberghs et al. (2019), Mercogliano et al. (2021) and Yan et al. (2020) were downloaded from the Copernicus Climate Change Service (C3S) (2023).

The results contain modified Copernicus Climate Change Service information 2023. Neither the European Commission nor ECMWF is responsible for any use that may be made of the Copernicus information or data it contains.

This publication has been prepared using European Union's Copernicus Land Monitoring Service information (<https://doi.org/10.2909/debc1869-a4a2-4611-ae95-daeefce23490>).

## References

- Abadie, L., 2017. Sea level damage risk with probabilistic weighting of IPCC scenarios: an application to major coastal cities. *J. Clean. Prod.* 175 <https://doi.org/10.1016/j.jclepro.2017.11.069>.
- Adger, W.N., Dessai, S., Goulden, M., Hulme, M., Lorenzoni, I., Nelson, D.R., Naess, L.O., Wolf, J., Wreford, A., 2009. Are there social limits to adaptation to climate change? *Clim. Change* 93, 335–354. <https://doi.org/10.1007/s10584-008-9520-z>.
- Adger, W.N., Huq, S., Brown, K., Conway, D., Hulme, M., 2003. Adaptation to climate change in the developing world. *Prog. Dev. Stud.* 3, 179–195. <https://doi.org/10.1191/1464993403ps0600a>.
- Aerts, J.C.J.H., Wouter, B.W.J., Kerry, E., Ning, L., Hans, de M., O, M.-K.E., 2014a. Evaluating flood resilience strategies for coastal megacities. *Science* 344, 473–475. <https://doi.org/10.1126/science.1248222>.
- Aerts, J.C.J.H., Wouter, B.W.J., Kerry, E., Ning, L., Hans, de M., O, M.-K.E., 2014b. Evaluating flood resilience strategies for coastal megacities. *Science* 344, 473–475. <https://doi.org/10.1126/science.1248222>.
- Alessandrini, V., Bertoni, D., Rangel-Buitrago, N., Ciccarelli, D., 2024. Implementing a vegetation-based risk index to support management actions in Mediterranean coastal dunes. *Ocean Coast Manag.* 252, 107105 <https://doi.org/10.1016/j.ocecoaman.2024.107105>.
- Almar, R., Ranasinghe, R., Bergsma, E.W.J., Diaz, H., Melet, A., Papa, F., Voudoukas, M., Athanasiou, P., Dada, O., Almeida, L.P., Kestenare, E., 2021.

- A global analysis of extreme coastal water levels with implications for potential coastal overtopping. *Nat. Commun.* 12, 3775. <https://doi.org/10.1038/s41467-021-24008-9>.
- Antunes, C., Rocha, C., Catita, C., 2019. Coastal flood assessment due to sea level rise and extreme storm events: a case study of the Atlantic coast of Portugal's mainland. *Geosciences* 9. <https://doi.org/10.3390/geosciences9050239>.
- Araya-Muñoz, D., Metzger, M.J., Stuart, N., Wilson, A.M.W., Carvajal, D., 2017. A spatial fuzzy logic approach to urban multi-hazard impact assessment in Concepción, Chile. *Sci. Total Environ.* 576, 508–519. <https://doi.org/10.1016/j.scitotenv.2016.10.077>.
- Argyroudis, S.A., Mitoulis, S.A., Chatzi, E., Baker, J.W., Brilakis, I., Gkoumas, K., Voudoukas, M., Hynes, W., Carluccio, S., Keou, O., Frangopol, D.M., Linkov, I., 2022. Digital technologies can enhance climate resilience of critical infrastructure. *Clim. Risk Manag.* 35, 100387 <https://doi.org/10.1016/j.crm.2021.100387>.
- Ashrafuol Islam, Md, Mitra, D., Dewan, A., Akhter, S.H., 2016. Coastal multi-hazard vulnerability assessment along the Ganges deltaic coast of Bangladesh—A geospatial approach. *Ocean Coast Manag.* 127, 1–15. <https://doi.org/10.1016/j.ocecoaman.2016.03.012>.
- Assem, H., Ghariba, S., Makrai, G., Johnston, P., Gill, L., Pilla, F., 2017. Urban water flow and water level prediction based on deep learning. In: Altun, Y., Das, K., Mielikäinen, T., Malerba, D., Stefanowski, J., Read, J., Žitnik, M., Ceci, M., Džeroski, S. (Eds.), *Machine Learning and Knowledge Discovery in Databases*. Springer International Publishing, Cham, pp. 317–329.
- Aznar-Siguán, G., Bresch, D.N., 2019. CLIMADA v1: a global weather and climate risk assessment platform. *Geosci. Model Dev. (GMD)* 12, 3085–3097. <https://doi.org/10.5194/gmd-12-3085-2019>.
- B, L.A., Erin, S., Khairul, I., Sara, S., Joanne, S., J, S.R., P, M.S., Paul, K., Kristin, T., W, S. M., 2023. Perspectives and propositions on resilience as interdisciplinary, multilevel, and interdependent. *Nat. Hazards Rev.* 24, 03123004 <https://doi.org/10.1061/NHREFO.NHENG-1471>.
- Bagdanavičiūtė, I., Kelpšaitė-Rimkienė, L., Galiniene, J., Soomere, T., 2019. Index based multi-criteria approach to coastal risk assessment. *J. Coast Conserv.* 23, 785–800. <https://doi.org/10.1007/s11852-018-0638-5>.
- Barzokhar, M., Parnell, K.E., Soomere, T., Dragovich, D., Engström, J., 2021. Decision support tools, systems and indices for advanced coastal planning and management: a review. *Ocean Coast Manag.* 212, 105813 <https://doi.org/10.1016/j.ocecoaman.2021.105813>.
- Beden, N., Ulke, A., 2020. Flood hazard assessment of a flood-prone intensively urbanized area—A case study from Samsun Province, Turkey. *Geofizika* 37, 2020. <https://doi.org/10.15233/gfz.2020.37.2>.
- Bergillos, R.J., Rodríguez-Delgado, C., Medina, L., Iglesias, G., 2020. Coastal cliff exposure and management. *Ocean Coast Manag.* 198, 105387 <https://doi.org/10.1016/j.ocecoaman.2020.105387>.
- Berrang-Ford, L., Siders, A.R., Lesnikowski, A., Fischer, A.P., Callaghan, M.W., Haddaway, N.R., Mach, K.J., Araos, M., Shah, M.A.R., Wannowitz, M., Doshi, D., Leiter, T., Matavel, C., Musah-Surug, J.I., Wong-Parodi, G., Antwi-Agyei, P., Ajibade, I., Chauhan, N., Kakenmaster, W., Grady, C., Chalastani, V.I., Jagannathan, K., Galappaththi, E.K., Sitati, A., Scarpa, G., Totin, E., Davis, K., Hamilton, N.C., Kirchhoff, C.J., Kumar, P., Pentz, B., Simpson, N.P., Theokritoff, E., Deryng, D., Reckien, D., Zavaleta-Cortijo, C., Ulibarri, N., Segnon, A.C., Khavhagali, V., Shang, Y., Zvobgo, L., Zommers, Z., Xu, J., Williams, P.A., Canosa, I. V., van Maanen, N., van Bavel, B., van Aalst, M., Turek-Hankins, L.L., Trivedi, H., Trisos, C.H., Thomas, A., Thakur, S., Templeman, S., Stringer, L.C., Sotnik, G., Sjöstrom, K.D., Singh, C., Siña, M.Z., Shukla, R., Sardans, J., Salubi, E.A., Safaei Chalkasra, L.S., Ruiz-Díaz, R., Richards, C., Pokharel, P., Petzold, J., Penuelas, J., Pelaez Avila, J., Murillo, J.B.P., Ouni, S., Niemann, J., Nielsen, M., New, M., Nayna Scherdtle, P., Nagle Alverio, G., Mullin, C.A.G., Mullenite, J., Mosurska, A., Morecroft, M.D., Minx, J.C., Maskell, G., Nunbogu, A.M., Magnan, A.K., Lwasa, S., Lukas-Sithole, M., Lissner, T., Lilford, O., Koller, S.F., Jurjonas, M., Joe, E.T., Huynh, L.T.M., Hill, A., Hernandez, R.R., Hegde, G., Hawxwell, T., Harper, S., Harden, A., Haasnoot, M., Gilmore, E.A., Gichuki, L., Gatt, A., Garschagen, M., Ford, J.D., Forbes, A., Farrell, A.D., Enquist, C.A.F., Elliott, S., Duncan, E., Coughlan de Perez, E., Coggins, S., Chen, T., Campbell, D., Browne, K.E., Bowen, K.E., Biesbroek, R., Bhatt, I.D., Bezner Kerr, R., Barr, S.L., Baker, E., Austin, S.E., Arotoma-Rojas, I., Anderson, C., Ajaz, W., Agrawal, T., Abu, T.Z., 2021. A systematic global stocktake of evidence on human adaptation to climate change. *Nat. Clim. Change* 11, 989–1000. <https://doi.org/10.1038/s41558-021-01170-y>.
- Binita, K.C., Shepherd, J.M., King, A.W., Johnson Gaither, C., 2021. Multi-hazard climate risk projections for the United States. *Nat. Hazards* 105, 1963–1976. <https://doi.org/10.1007/s11069-020-04385-y>.
- Birkmann, J., Dech, S.W., Hürzinger, G., Klein, R., Klüpfel, H., Lehmann, F., Mott, C., Nagel, K., Schlurmann, T., Setiadi, N.J., Siegfert, F., Strunz, G., 2006. *Measuring Vulnerability to Promote Disaster-Resilient Societies: Conceptual Frameworks and Definitions*.
- Blythe, J., Armitage, D., Alonso, G., Campbell, D., Esteves Dias, A.C., Epstein, G., Marschke, M., Nayak, P., 2020. Frontiers in coastal well-being and ecosystem services research: a systematic review. *Ocean Coast Manag.* 185, 105028 <https://doi.org/10.1016/j.ocecoaman.2019.105028>.
- Caires, S., Yan, K., 2020. Ocean surface wave indicators for the European coast from 1977 to 2100 derived from climate projections. *Copernicus Clim. Change Serv. (C3S) Clim. Data Store (CDS)*. <https://doi.org/10.24381/cds.1a072dd6> [WWW Document].
- Chang, H., Pallathadka, A., Sauer, J., Grimm, N.B., Zimmerman, R., Cheng, C., Iwaniec, D.M., Kim, Y., Lloyd, R., McPhearson, T., Rosenzweig, B., Troxler, T., Welty, C., Brenner, R., Herreros-Cantis, P., 2021. Assessment of urban flood vulnerability using the social-ecological-technological systems framework in six US cities. *Sustain. Cities Soc.* 68, 102786 <https://doi.org/10.1016/j.scs.2021.102786>.
- Chang, S., Mcdaniels, T., Fox, J., Dhariwal, R., Longstaff, H., 2013. Toward disaster-resilient cities: characterizing resilience of infrastructure systems with expert judgments. *Risk Anal.* 34 <https://doi.org/10.1111/risa.12133>.
- Chen, W., Huang, H., Dong, J., Zhang, Y., Tian, Y., Yang, Z., 2018. Social functional mapping of urban green space using remote sensing and social sensing data. *ISPRS J. Photogrammetry Remote Sens.* 146, 436–452. <https://doi.org/10.1016/j.isprsjprs.2018.10.010>.
- Colten, C.E., Glavovic, B.C., Hemmerling, S.A., 2022. Editorial: coastal cities in a changing climate. *Front. Environ. Sci.* 10 <https://doi.org/10.3389/fenvs.2022.878888>.
- Copernicus Climate Change Service, Climate Data Store, 2022. Winter windstorm indicators for Europe from 1979 to 2021 derived from reanalysis. *Copernicus Clim. Change Serv. (C3S) Clim. Data Store (CDS)*. <https://doi.org/10.24381/cds.9b4ea013> [WWW Document].
- Copernicus land monitoring service. *Urban Atlas, 2012*. <https://doi.org/10.2909/debc1869-a4a2-4611-ae95-daeefce23490> [WWW Document].
- Costa, Y., Martins, I., de Carvalho, G.C., Barros, F., 2023. Trends of sea-level rise effects on estuaries and estimates of future saline intrusion. *Ocean Coast Manag.* 236, 106490 <https://doi.org/10.1016/j.ocecoaman.2023.106490>.
- Crespi, A., Terzi, S., Cocuccioni, S., Zebisch, M., Berckmans, J., Füssel, H.-M., 2020. "Climate-related hazard indices for Europe". European topic centre on climate change impacts. *Vulnerabil. Adapt. Technol. Paper*. [https://doi.org/10.25424/cmcc/climate\\_related\\_hazard\\_indices\\_europe\\_2020](https://doi.org/10.25424/cmcc/climate_related_hazard_indices_europe_2020).
- Cutter, S.L., Boruff, B.J., Shirley, W.L., 2003. Social vulnerability to environmental hazards. *Soc. Sci. Q.* 84, 242–261.
- De Angeli, S., D'Andrea, M., Cazzola, G., Dolia, D., Duo, E., Rebora, N., 2018. Coastal Risk Assessment Framework: Comparison of modelled fluvial and marine inundation impacts, Bocca di Magra, Ligurian coast, Italy. *Coast Eng.* 134, 229–240. <https://doi.org/10.1016/j.coastaleng.2017.09.011>.
- de Burgh-Day, C.O., Leeuwenburg, T., 2023. Machine learning for numerical weather and climate modelling: a review. *Geosci. Model Dev. (GMD)* 16, 6433–6477. <https://doi.org/10.5194/gmd-16-6433-2023>.
- Debaine, F., Robin, M., 2012. A new GIS modelling of coastal dune protection services against physical coastal hazards. *Ocean Coast Manag.* 63, 43–54. <https://doi.org/10.1016/j.ocecoaman.2012.03.012>.
- Devoy, R., 2009. Coastal vulnerability and the implications of Sea-Level rise for Ireland. *J. Coast Res.* 24, 325–341. <https://doi.org/10.2112/07A-0007.1>.
- Di Napoli, M., Di Martire, D., Bausilio, G., Calcaterra, D., Confuorto, P., Firpo, M., Pepe, G., Cevasco, A., 2021. Rainfall-induced shallow landslide detachment, transit and runoff susceptibility mapping by integrating machine learning techniques and GIS-based approaches. *Water* 13. <https://doi.org/10.3390/w13040488>.
- Dottori, F., Alfieri, L., Bianchi, A., Skoien, J., Salamon, P., 2021. *River Flood Hazard Maps for Europe and the Mediterranean Basin Region*.
- Elliott, M., Cutts, N.D., Trono, A., 2014. A typology of marine and estuarine hazards and risks as vectors of change: a review for vulnerable coasts and their management. *Ocean Coast Manag.* 93, 88–99. <https://doi.org/10.1016/j.ocecoaman.2014.03.014>.
- Elmqvist, T., Andersson, E., Frantzeskaki, N., McPhearson, T., Olsson, P., Gaffney, O., Takeuchi, K., Folke, C., 2019. Sustainability and resilience for transformation in the urban century. *Nat. Sustain.* 2, 267–273. <https://doi.org/10.1038/s41893-019-0250-1>.
- Elrick-Barr, C.E., Thomsen, D.C., Smith, T.F., 2024. Governance innovations in the coastal zone: towards social-ecological resilience. *Environ Sci Policy* 153, 103687. <https://doi.org/10.1016/j.envsci.2024.103687>.
- Espinosa, L.A., Portela, M.M., 2022. Grid-point rainfall trends, teleconnection patterns, and regionalised droughts in Portugal (1919–2019). *Water* 14. <https://doi.org/10.3390/w14121863>.
- Espinosa, L.A., Portela, M.M., Matos, J.P., Gharbia, S., 2022. Climate change trends in a European coastal metropolitan area: rainfall, temperature, and extreme events (1864–2021). *Atmosphere* 13. <https://doi.org/10.3390/atmos13121995>.
- European Commission, Joint Research Centre (JRC), 2021. GDO standardized precipitation index GPCC, 3-month accumulation period (SPI-3) (version 1.2.0) [WWW Document]. European Commission, Joint Research Centre (JRC). <http://data.europa.eu/89h/dca55d34-9151-419d-9366-5d64c28a4e07>.
- Fang, J., Lincke, D., Brown, S., Nicholls, R.J., Wolff, C., Merckens, J.-L., Hinkel, J., Vafeidis, A.T., Shi, P., Liu, M., 2020. Coastal flood risks in China through the 21st century — an application of DIVA. *Sci. Total Environ.* 704, 135311 <https://doi.org/10.1016/j.scitotenv.2019.135311>.
- Fitton, J.M., Addo, K.A., Jayson-Quashigah, P.-N., Nagy, G.J., Gutiérrez, O., Panario, D., Carro, I., Seijo, L., Segura, C., Verocai, J.E., Luoma, S., Klein, J., Zhang, T.-T., Birchall, J., Stempel, P., 2021. Challenges to climate change adaptation in coastal small towns: examples from Ghana, Uruguay, Finland, Denmark, and Alaska. *Ocean Coast Manag.* 212, 105787 <https://doi.org/10.1016/j.ocecoaman.2021.105787>.
- Flood, S., Schechtman, J., 2014. The rise of resilience: evolution of a new concept in coastal planning in Ireland and the US. *Ocean Coast Manag.* 102, 19–31. <https://doi.org/10.1016/j.ocecoaman.2014.08.015>.
- Forzieri, G., Cescatti, A., e Silva, F.B., Feyen, L., 2017. Increasing risk over time of weather-related hazards to the European population: a data-driven prognostic study. *Lancet Planet. Health* 1, e200–e208. [https://doi.org/10.1016/S2542-5196\(17\)30082-7](https://doi.org/10.1016/S2542-5196(17)30082-7).
- Frazier, T.G., Thompson, C.M., Dezzani, R.J., Butsick, D., 2013. Spatial and temporal quantification of resilience at the community scale. *Appl. Geogr.* 42, 95–107. <https://doi.org/10.1016/j.apgeog.2013.05.004>.
- Gallina, V., Torresan, S., Critto, A., Sperotto, A., Glade, T., Marcomini, A., 2016. A review of multi-risk methodologies for natural hazards: consequences and challenges for a climate change impact assessment. *J. Environ. Manag.* 168, 123–132. <https://doi.org/10.1016/j.jenvman.2015.11.011>.

- Garner, G.G., Hermans, T., Kopp, R.E., Slangen, A.B.A., Edwards, T.L., Levermann, A., Nowicki, S., Palmer, M.D., Smith, C., Fox-Kemper, B., Hewitt, H.T., Xiao, C., Adalgerdóttir, G., Drifflou, S.S., Edwards, T.L., Golledge, N.R., Hemer, M., Krinner, G., Mix, A., Notz, D., Nurhati, I.S., Ruiz, L., Sallée, J.-B., Yu, Y., Hua, L., Palmer, T., Pearson, B., 2021. IPCC AR6 Sea-Level rise projections [WWW Document]. URL: <https://podaac.jpl.nasa.gov/announcements/2021-08-09-Sea-level-1-projections-from-the-IPCC-6th-Assessment-Report>. (Accessed 27 July 2023).
- Glavovic, B.C., Smith, T.F., White, I., 2022. The tragedy of climate change science. *Clim. Dev.* 14, 829–833. <https://doi.org/10.1080/17565529.2021.2008855>.
- Godwyn-Paulson, P., Jonathan, M.P., Rodríguez-Espinosa, P.F., Abdul Rahaman, S., Roy, P.D., Muthusankar, G., Lakshumanan, C., 2022. Multi-hazard risk assessment of coastal municipalities of Oaxaca, Southwestern Mexico: an index based remote sensing and geospatial technique. *Int. J. Disaster Risk Reduc.* 77, 103041 <https://doi.org/10.1016/j.ijdrr.2022.103041>.
- Grosso, N., Dias, L., Costa, H.P., Santos, F.D., Garrett, P., 2015. Continental Portuguese territory flood social susceptibility index. *Nat. Hazards Earth Syst. Sci.* 15, 1921–1931. <https://doi.org/10.5194/nhess-15-1921-2015>.
- Hagenlocher, M., Renaud, F.G., Haas, S., Sebesvari, Z., 2018. Vulnerability and risk of deltaic social-ecological systems exposed to multiple hazards. *Sci. Total Environ.* 631–632, 71–80. <https://doi.org/10.1016/j.scitotenv.2018.03.013>.
- Hay, C.C., Morrow, E., Kopp, R.E., Mitrovica, J.X., 2015. Probabilistic reanalysis of twentieth-century sea-level rise. *Nature* 517, 481–484. <https://doi.org/10.1038/nature14093>.
- Hersbach, H., Bell, B., Berrisford, P., Hirahara, S., Horányi, A., Muñoz-Sabater, J., Nicolas, J., Peubey, C., Radu, R., Schepers, D., Simmons, A., Soci, C., Abdalla, S., Abellan, X., Balsamo, G., Bechtold, P., Biavati, G., Bidlot, J., Bonavita, M., De Chiara, G., Dahlgren, P., Dee, D., Diamantakis, M., Dragani, R., Flemming, J., Forbes, R., Fuentes, M., Geer, A., Haimberger, L., Healy, S., Hogan, R.J., Hólm, E., Janisková, M., Keeley, S., Laloyaux, P., Lopez, P., Lupu, C., Radnoti, G., de Rosnay, P., Rozum, I., Vamborg, F., Villaume, S., Thépaut, J.-N., 2020. The ERA5 global reanalysis. *Q. J. R. Meteorol. Soc.* 146, 1999–2049. <https://doi.org/10.1002/qj.3803>.
- Hinks, S., Carter, J., Connelly, A., 2023. A new typology of climate change risk for European cities and regions: principles and applications. *Global Environ. Change* 83, 102767. <https://doi.org/10.1016/j.gloenvcha.2023.102767>.
- Hinkel, J., Klein, R., 2009. Integrating knowledge to assess coastal vulnerability to sea-level rise: the development of the DIVA tool. *Global Environ. Change* 19, 384–395. <https://doi.org/10.1016/j.gloenvcha.2009.03.002>.
- Holand, I.S., Lujala, P., Rød, J.K., 2011. Social vulnerability assessment for Norway: a quantitative approach. *Geografisk Tidsskrift* 65, 1–17. <https://doi.org/10.1080/00291951.2010.550167>.
- Hooyberghs, H., Berckmans, J., Lefebvre, F., De Ridder, K., 2019. Heat waves and cold spells in Europe derived from climate projections. *Copernicus Clim. Change Serv. (C3S) Clim. Data Store (CDS)*. <https://doi.org/10.24381/cds.9e7ca677> [WWW Document].
- Hu, J., Zhou, Y., Yang, Y., Chen, G., Chen, W., Hejazi, M., 2023. Multi-city assessments of human exposure to extreme heat during heat waves in the United States. *Remote Sens. Environ.* 295, 113700 <https://doi.org/10.1016/j.rse.2023.113700>.
- Hwang, C.-L., Yoon, K., 2012. *Multiple Attribute Decision Making: Methods and Applications a State-Of-The-Art Survey*. Springer Science & Business Media.
- Intergovernmental Panel on Climate Change (IPCC), 2023. Ocean, cryosphere and sea level change. In: *Climate Change 2021 – the Physical Science Basis: Working Group I Contribution to the Sixth Assessment Report of the Intergovernmental Panel on Climate Change*. Cambridge University Press, Cambridge, pp. 1211–1362. <https://doi.org/10.1017/9781009157896.011>.
- IPCC, F.C.B., 2014. *Climate change 2014: impacts, adaptation, and vulnerability. Part A: global and sectoral aspects. Contribution of Working Group II to the fifth assessment report of the Intergovernmental Panel on Climate Change*. *Clim. Change*.
- Jeffers, J.M., 2014. Environmental knowledge and human experience: using a historical analysis of flooding in Ireland to challenge contemporary risk narratives and develop creative policy alternatives. *Environ. Res. Lett.* 13, 229–247. <https://doi.org/10.1080/17477891.2014.902800>.
- Jeffers, J.M., 2011. The Cork City flood of November 2009: lessons for flood risk management and climate change adaptation at the urban scale. *Ir. Geogr.* 44, 61–80. <https://doi.org/10.1080/00750778.2011.615283>.
- Jones, B., O'Neill, B.C., 2016. Spatially explicit global population scenarios consistent with the Shared Socioeconomic Pathways. *Environ. Res. Lett.* 11, 084003 <https://doi.org/10.1088/1748-9326/11/8/084003>.
- Kappes, M.S., Keiler, M., von Elverfeldt, K., Glade, T., 2012. Challenges of analyzing multi-hazard risk: a review. *Nat. Hazards* 64, 1925–1958. <https://doi.org/10.1007/s11069-012-0294-2>.
- Kerguillac, R., Audère, M., Baltzer, A., Debaine, F., Fattal, P., Juigner, M., Launeau, P., Le Mauff, B., Luquet, F., Maanan, M., Pouzet, P., Robin, M., Rollo, N., 2019. Monitoring and management of coastal hazards: Creation of a regional observatory of coastal erosion and storm surges in the pays de la Loire region (Atlantic coast, France). *Ocean Coast Manag.* 181, 104904 <https://doi.org/10.1016/j.ocecoaman.2019.104904>.
- Kirezci, E., Young, I.R., Ranasinghe, R., Muis, S., Nicholls, R.J., Lincke, D., Hinkel, J., 2020. Projections of global-scale extreme sea levels and resulting episodic coastal flooding over the 21st Century. *Sci. Rep.* 10, 11629 <https://doi.org/10.1038/s41598-020-67736-6>.
- Klein, R.J.T., Nicholls, R.J., 1999. *Assessment of coastal vulnerability to climate change*. *Ambio* 28, 182–187.
- Kleinschroth, F., Savilaakso, S., Kowarik, I., Martínez, P.J., Chang, Y., Jakstis, K., Schneider, J., Fischer, L.K., 2024. Global disparities in urban green space use during the COVID-19 pandemic from a systematic review. *Nature Cities* 1, 136–149. <https://doi.org/10.1038/s44284-023-00020-6>.
- Koks, E.E., Rozenberg, J., Zorn, C., Tariverdi, M., Voudoukas, M., Fraser, S.A., Hall, J. W., Hallegatte, S., 2019. A global multi-hazard risk analysis of road and railway infrastructure assets. *Nat. Commun.* 10, 2677. <https://doi.org/10.1038/s41467-019-10442-3>.
- Kopp, R., Garner, G., Hermans, T., Jha, S., Kumar, P., Slangen, A., Turilli, M., Edwards, T., Gregory, J., Koubbe, G., Levermann, A., Merzky, A., Nowicki, S., Palmer, M., Smith, C., 2023. The Framework for Assessing Changes to Sea-level (FACTS) v1.0-rc: a platform for characterizing parametric and structural uncertainty in future global, relative, and extreme sea-level change. <https://doi.org/10.5194/egusphere-2023-14>.
- Kovats, S., Valentini, R., Bouwer, L., Georgopoulou, E., Jacob, D., Martin, E., Rounsevell, M., Soussana, J.-F., 2014. Europe 1267–1326. <https://doi.org/10.1017/CBO9781107415386.003>.
- Kulp, S.A., Strauss, B.H., 2019. New elevation data triple estimates of global vulnerability to sea-level rise and coastal flooding. *Nat. Commun.* 10, 4844. <https://doi.org/10.1038/s41467-019-12808-z>.
- Kumar, S., Tiwari, P., Zymbler, M., 2019. Internet of Things is a revolutionary approach for future technology enhancement: a review. *J. Big Data* 6, 111. <https://doi.org/10.1186/s40537-019-0268-2>.
- Laino, E., Iglesias, G., 2024. Multi-hazard assessment of climate-related hazards for European coastal cities. *J. Environ. Manag.* 357, 120787 <https://doi.org/10.1016/j.jenvman.2024.120787>.
- Laino, E., Iglesias, G., 2023a. High-level characterisation and mapping of key climate-change hazards in European coastal cities. *Nat. Hazards*. <https://doi.org/10.1007/s11069-023-06349-4>.
- Laino, E., Iglesias, G., 2023b. Extreme climate change hazards and impacts on European coastal cities: a review. *Renew. Sustain. Energy Rev.* 184, 113587 <https://doi.org/10.1016/j.rser.2023.113587>.
- Laino, E., Iglesias, G., 2023c. Scientometric review of climate-change extreme impacts on coastal cities. *Ocean Coast Manag.* 242, 106709 <https://doi.org/10.1016/j.ocecoaman.2023.106709>.
- Laino, E., Paranzunzio, R., Iglesias, G., 2024. Scientometric review on multiple climate-related hazards indices. *Sci. Total Environ.*, 174004 <https://doi.org/10.1016/j.scitotenv.2024.174004>.
- Laurien, F., Martin, J.G.C., Mehryar, S., 2022. Climate and disaster resilience measurement: persistent gaps in multiple hazards, methods, and practicability. *Clim. Risk Manag.* 37, 100443 <https://doi.org/10.1016/j.crm.2022.100443>.
- Lavaysse, C., Cammalleri, C., Dosio, A., van der Schrier, G., Toreti, A., Vogt, J., 2018. Towards a monitoring system of temperature extremes in Europe. *Nat. Hazards Earth Syst. Sci.* 18, 91–104. <https://doi.org/10.5194/nhess-18-91-2018>.
- Leahy, P.G., Kiely, G., 2011. Short duration rainfall extremes in Ireland: influence of climatic variability. *Water Resour. Manag.* 25, 987–1003. <https://doi.org/10.1007/s11269-010-9737-2>.
- Lehmann, M., Major, D.C., Fitton, J., Doust, K., O'Donoghue, S., 2021. The way forward: supporting climate adaptation in coastal towns and small cities. *Ocean Coast Manag.* 212, 105785 <https://doi.org/10.1016/j.ocecoaman.2021.105785>.
- Lenôtre, N., Thierry, P., Batkowski, D., Vermeersch, F., 2004. *EUROSION Project the Coastal Erosion Layer WP 2.6 BRGM/PC-52864-FR*, p. 45, 8 fig., 3 app.
- Li, X., Zhou, Y., Hejazi, M., Wise, M., Vernon, C., Iyer, G., Chen, W., 2021. Global urban growth between 1870 and 2100 from integrated high resolution mapped data and urban dynamic modeling. *Commun Earth Environ* 2, 201. <https://doi.org/10.1038/s43247-021-00273-w>.
- Lima, C.O., Bonetti, J., 2020. Bibliometric analysis of the scientific production on coastal communities' social vulnerability to climate change and to the impact of extreme events. *Nat. Hazards* 102, 1589–1610. <https://doi.org/10.1007/s11069-020-03974-1>.
- Losada, I.J., Toimil, A., Muñoz, A., Garcia-Fletcher, A.P., Diaz-Simal, P., 2019. A planning strategy for the adaptation of coastal areas to climate change: the Spanish case. *Ocean Coast Manag.* 182, 104983 <https://doi.org/10.1016/j.ocecoaman.2019.104983>.
- Lückenköter, J., Lindner, C., Greiving, S., 2013. Overall impact and vulnerability to climate change in Europe. In: *European Climate Vulnerabilities and Adaptation*, pp. 147–169. <https://doi.org/10.1002/9781118474822.ch9>.
- Lung, T., Lavalle, C., Hiederer, R., Dosio, A., Bouwer, L.M., 2013. A multi-hazard regional level impact assessment for Europe combining indicators of climatic and non-climatic change. *Global Environ. Change* 23, 522–536. <https://doi.org/10.1016/j.gloenvcha.2012.11.009>.
- MacManus, K., Balk, D., Engin, H., McGranahan, G., Inman, R., 2021. Estimating population and urban areas at risk of coastal hazards, 1990–2015: how data choices matter. *Earth Syst. Sci. Data* 13, 5747–5801. <https://doi.org/10.5194/essd-13-5747-2021>.
- Magarotto, M., Deus, R., Costa, M., Masanet, E., 2017. Green areas in coastal cities – conflict of interests or stakeholders' perspectives? *Int. J. Sustain. Dev. Plann.* 12, 1260–1271. <https://doi.org/10.2495/SDP-V12-N8-1260-1271>.
- Maloutas, T., 2024. The role of vertical segregation in urban social processes. *Nature Cities* 1, 185–193. <https://doi.org/10.1038/s44284-024-00037-5>.
- Martins, D.S., Razieli, T., Paulo, A.A., Pereira, L.S., 2012. Spatial and temporal variability of precipitation and drought in Portugal. *Nat. Hazards Earth Syst. Sci.* 12, 1493–1501. <https://doi.org/10.5194/nhess-12-1493-2012>.
- McClatchey, J., Devoy, R., Woolf, D., Bremner, B., James, N., 2014. Climate change and adaptation in the coastal areas of Europe's Northern Periphery Region. *Ocean Coast Manag.* 94, 9–21. <https://doi.org/10.1016/j.ocecoaman.2014.03.013>.

- McEvoy, S., Haasnoot, M., Biesbroek, R., 2021. How are European countries planning for sea level rise? *Ocean Coast Manag.* 203, 105512 <https://doi.org/10.1016/j.ocecoaman.2020.105512>.
- McKee, T., Doesken, N., Kleist, J., 1993. The relationship of drought frequency and duration to time scales. In: *Paper Presented at 8th Conference on Applied Climatology*, vol. 17. Am. Meteorol. Soc., Anaheim, Calif.
- McKinley, E., Crowe, P.R., Stori, F., Ballinger, R., Brew, T.C., Blacklaw-Jones, L., Cameron-Smith, A., Crowley, S., Cocco, C., O'Mahony, C., McNally, B., Power, P., Foley, K., 2021. 'Going digital' - lessons for future coastal community engagement and climate change adaptation. *Ocean Coast Manag.* 208, 105629 <https://doi.org/10.1016/j.ocecoaman.2021.105629>.
- Measham, T.G., Preston, B.L., Smith, T.F., Brooke, C., Gorddard, R., Withycombe, G., Morrison, C., 2011. Adapting to climate change through local municipal planning: barriers and challenges. *Mitig. Adapt. Strategies Glob. Change* 16, 889–909. <https://doi.org/10.1007/s11027-011-9301-2>.
- Mercogliano, P., Rianna, G., Reeder, A., Raffa, M., Mancini, M., Stojilkovic, M., de Valk, C., van der Schrier, G., 2021. Extreme precipitation risk indicators for Europe and European cities from 1950 to 2019. *Copernicus Clim. Change Serv. (C3S) Clim. Data Store (CDS)*. <https://doi.org/10.24381/cds.3a9c4f89> [WWW Document].
- Merkens, J.-L., Reimann, L., Hinkel, J., Vafeidis, A.T., 2016. Gridded population projections for the coastal zone under the Shared Socioeconomic Pathways. *Global Planet. Change* 145, 57–66. <https://doi.org/10.1016/j.gloplacha.2016.08.009>.
- Mitsopoulos, I., Mallinis, G., 2017. A data-driven approach to assess large fire size generation in Greece. *Nat. Hazards* 88, 1591–1607. <https://doi.org/10.1007/s11069-017-2934-z>.
- Moradian, S., AghaKouchak, A., Gharbia, S., Broderick, C., Olbert, A.I., 2024. Forecasting of compound ocean-fluvial floods using machine learning. *J. Environ. Manag.* 364, 121295 <https://doi.org/10.1016/j.jenvman.2024.121295>.
- Moradian, S., Iglesias, G., Broderick, C., Olbert, I.A., 2023. Assessing the impacts of climate change on precipitation through a hybrid method of machine learning and discrete wavelet transform techniques, case study: Cork, Ireland. *J. Hydrol. Reg. Stud.* 49, 101523. <https://doi.org/10.1016/j.ejrh.2023.101523>.
- Murray, A.T., Carvalho, L., Church, R.L., Jones, C., Roberts, D., Xu, J., Zigner, K., Nash, D., 2021. Coastal vulnerability under extreme weather. *Appl Spat Anal. Pol.* 14, 497–523. <https://doi.org/10.1007/s12061-020-09357-0>.
- Neumann, B., Vafeidis, A.T., Zimmermann, J., Nicholls, R.J., 2015. Future coastal population growth and exposure to sea-level rise and coastal flooding—a global assessment. *PLoS One* 10, e0118571. <https://doi.org/10.1371/journal.pone.0118571>.
- Nguyen, T.T.X., Bonetti, J., Rogers, K., Woodroffe, C.D., 2016. Indicator-based assessment of climate-change impacts on coasts: a review of concepts, methodological approaches and vulnerability indices. *Ocean Coast Manag.* 123, 18–43. <https://doi.org/10.1016/j.ocecoaman.2015.11.022>.
- Owolabi, T.A., Sajjad, M., 2023. A global outlook on multi-hazard risk analysis: a systematic and scientometric review. *Int. J. Disaster Risk Reduc.* 92, 103727 <https://doi.org/10.1016/j.ijdrr.2023.103727>.
- Pal, I., Kumar, A., Mukhopadhyay, A., 2023. Risks to coastal critical infrastructure from climate change. *Annu. Rev. Environ. Resour.* 48 <https://doi.org/10.1146/annurev-environ-112320-101903>.
- Pant, R., Hall, J.W., Blainey, S.P., 2016. Vulnerability assessment framework for interdependent critical infrastructures: case-study for Great Britain's rail network. *Eur. J. Transport Infrastruct. Res.* <https://doi.org/10.18757/EJTIR.2016.16.1.3120>.
- Paranunzio, R., Anton, I., Adirosi, E., Ahmed, T., Baldini, L., Brandini, C., Giannetti, F., Meulenbergh, C., Ortolani, A., Pilla, F., Iglesias, G., Gharbia, S., 2024. A new approach towards a user-driven coastal climate service to enhance climate resilience in European cities. *Sustainability* 16. <https://doi.org/10.3390/su16010335>.
- Paranunzio, R., Dwyer, E., Fitton, J.M., Alexander, P.J., O'Dwyer, B., 2021. Assessing current and future heat risk in Dublin city, Ireland. *Urban Clim.* 40, 100983 <https://doi.org/10.1016/j.uclim.2021.100983>.
- Pelling, M., 2010. Adaptation to climate change: from resilience to transformation. *Adaptation Clim. Change: Resilience Transformat.* <https://doi.org/10.4324/9780203889046>.
- Petrosillo, I., Zurlini, G., Grato, E., Zaccarelli, N., 2006. Indicating fragility of socio-ecological tourism-based systems. *Ecol. Indic.* 6, 104–113. <https://doi.org/10.1016/j.ecolind.2005.08.008>.
- Petzold, J., Ratter, B.M.W., 2015. Climate change adaptation under a social capital approach – an analytical framework for small islands. *Ocean Coast Manag.* 112, 36–43. <https://doi.org/10.1016/j.ocecoaman.2015.05.003>.
- Pourghasemi, H.R., Gayen, A., Panahi, M., Rezaie, F., Blaschke, T., 2019. Multi-hazard probability assessment and mapping in Iran. *Sci. Total Environ.* 692, 556–571. <https://doi.org/10.1016/j.scitotenv.2019.07.203>.
- Ranasinghe, R., Ruane, A.C., Vautard, R., Arnell, N., Coppola, E., Cruz, F.A., Dessai, S., Islam, A.S., Rahimi, M., Ruiz Carrascal, D., Sillmann, J., Sylla, M.B., Tebaldi, C., Wang, W., Zaaboul, R., 2021. Climate change information for regional impact and risk assessment. In: *Masson-Delmotte, V., Zhai, P., Pirani, A., Connors, S.L., Péan, C., Berger, S., Caud, N., Chen, Y., Goldfarb, L., Gomis, M.I., Huang, M., Leitzell, K., Lonnoy, E., Matthews, J.B.R., Maycock, T.K., Waterfield, T., Yelekçi, O., Yu, R., Zho, B. (Eds.), Climate Change 2021: The Physical Science Basis. Contribution of Working Group I to the Sixth Assessment Report of the Intergovernmental Panel on Climate Change*. Cambridge University Press.
- Rangel-Buitrago, N., Neal, W.J., de Jonge, V.N., 2020. Risk assessment as tool for coastal erosion management. *Ocean Coast Manag.* 186, 105099 <https://doi.org/10.1016/j.ocecoaman.2020.105099>.
- Riaz, K., McAfee, M., Gharbia, S.S., 2023. Management of climate resilience: exploring the potential of digital twin technology, 3D city modelling, and early warning systems. *Sensors* 23. <https://doi.org/10.3390/s23052659>.
- Rodriguez-Delgado, C., Bergillos, R.J., Iglesias, G., 2020. Coastal infrastructure operativity against flooding – a methodology. *Sci. Total Environ.* 719, 137452 <https://doi.org/10.1016/j.scitotenv.2020.137452>.
- Rodriguez-Delgado, C., Bergillos, R.J., Iglesias, G., 2019. An artificial neural network model of coastal erosion mitigation through wave farms. *Environ. Model. Software* 119, 390–399. <https://doi.org/10.1016/j.envsoft.2019.07.010>.
- Sacchini, A., Ferraris, F., Faccini, F., Firpo, M., 2012. Environmental climatic maps of Liguria (Italy). *J. Maps* 8, 199–207. <https://doi.org/10.1080/17445647.2012.703901>.
- Sahoo, B., Bhaskaran, P.K., 2018. Multi-hazard risk assessment of coastal vulnerability from tropical cyclones – a GIS based approach for the Odisha coast. *J. Environ. Manag.* 206, 1166–1178. <https://doi.org/10.1016/j.jenvman.2017.10.075>.
- Santos, J.F., Pulido-Calvo, I., Portela, M.M., 2010. Spatial and temporal variability of droughts in Portugal. *Water Resour. Res.* 46 <https://doi.org/10.1029/2009WR008071>.
- Sekovski, I., Del Rio, L., Armaroli, C., 2020. Development of a coastal vulnerability index using analytical hierarchy process and application to Ravenna province (Italy). *Ocean Coast Manag.* 183, 104982 <https://doi.org/10.1016/j.ocecoaman.2019.104982>.
- Spalding, M.D., Ruffo, S., Lacambra, C., Meliane, I., Hale, L.Z., Shepard, C.C., Beck, M. W., 2014. The role of ecosystems in coastal protection: adapting to climate change and coastal hazards. *Ocean Coast Manag.* 90, 50–57. <https://doi.org/10.1016/j.ocecoaman.2013.09.007>.
- Stanchev, H., Palazov, A., Stancheva, M., 2009. 3D GIS model for flood risk assessment of varna bay due to extreme sea level rise. *J. Coast Res.* 1597–1601.
- Stepanova, O., Bruckmeier, K., 2013. The relevance of environmental conflict research for coastal management. A review of concepts, approaches and methods with a focus on Europe. *Ocean Coast Manag.* 75, 20–32. <https://doi.org/10.1016/j.ocecoaman.2013.01.007>.
- Tang, Z., Dai, Z., Fu, X., Li, X., 2013. Content analysis for the U.S. coastal states' climate action plans in managing the risks of extreme climate events and disasters. *Ocean Coast Manag.* 80, 46–54. <https://doi.org/10.1016/j.ocecoaman.2013.04.004>.
- Thomas, A., Theokritoff, E., Lesnikowski, A., Reckien, D., Jagannathan, K., Cremades, R., Campbell, D., Joe, E.T., Sitati, A., Singh, C., Segnon, A.C., Pentz, B., Musah-Surugu, J.I., Mullin, C.A., Mach, K.J., Gichuki, L., Galappaththi, E., Chalastani, V.I., Ajibade, I., Ruiz-Diaz, R., Grady, C., Garschagen, M., Ford, J., Bowen, K., Team, G.A. M.I., 2021. Global evidence of constraints and limits to human adaptation. *Reg. Environ. Change* 21, 85. <https://doi.org/10.1007/s10113-021-01808-9>.
- Tiepolo, M., Bacci, M., Braccio, S., Bechis, S., 2019. Multi-hazard risk assessment at community level integrating local and scientific knowledge in the hodh chargui. *Mauritania. Sustainability* 11. <https://doi.org/10.3390/su11185063>.
- Tiwari, A., Rodrigues, L.C., Lucy, F.E., Gharbia, S., 2022. Building climate resilience in coastal city living Labs using ecosystem-based adaptation: a systematic review. *Sustainability* 14. <https://doi.org/10.3390/su141710863>.
- Toledo, I., Pagán, J.I., López, I., Aragonés, L., 2022. Causes of the different behaviour against erosion: study case of the Benidorm Beaches (1956–2021). *Mar. Georesour. Geotechnol.* 1–14. <https://doi.org/10.1080/1064119X.2022.2084003>.
- Valchev, N., Eftimova, P., Andreeva, N., 2018. Implementation and validation of a multi-domain coastal hazard forecasting system in an open bay. *Coast Eng.* 134, 212–228. <https://doi.org/10.1016/j.coastaleng.2017.08.008>.
- Venvik, G., Bang-Kittilsen, A., Boogaard, F.C., 2019. Risk assessment for areas prone to flooding and subsidence: a case study from Bergen, Western Norway. *Nord. Hydrol* 51, 322–338. <https://doi.org/10.2166/nh.2019.030>.
- Vesselinov, E., Villamizar-Santamaría, S.F., Gomez, C.J., Fernández, E.M., 2021. A global community or a global waste of time? Content analysis of the Facebook site "Humans of New York.". *J. Urban Aff.* 43, 117–139. <https://doi.org/10.1080/07352166.2019.1697184>.
- Vousdoukas, M.I., Mentaschi, L., Hinkel, J., Ward, P.J., Mongelli, I., Ciscar, J.-C., Feyen, L., 2020. Economic motivation for raising coastal flood defenses in Europe. *Nat. Commun.* 11, 2119. <https://doi.org/10.1038/s41467-020-15665-3>.
- Vousdoukas, M.I., Mentaschi, L., Voukouvalas, E., Verlaan, M., Feyen, L., 2017. Extreme sea levels on the rise along Europe's coasts. *Earth's Future* 5, 304–323. <https://doi.org/10.1002/2016EF000505>.
- Vousdoukas, M.I., Mentaschi, L., Voukouvalas, E., Verlaan, M., Jevrejeva, S., Jackson, L. P., Feyen, L., 2018. Global probabilistic projections of extreme sea levels show intensification of coastal flood hazard. *Nat. Commun.* 9, 2360. <https://doi.org/10.1038/s41467-018-04692-w>.
- Wahl, T., Haigh, I.D., Nicholls, R.J., Arns, A., Dangendorf, S., Hinkel, J., Slangen, A.B.A., 2017. Understanding extreme sea levels for broad-scale coastal impact and adaptation analysis. *Nat. Commun.* 8, 16075 <https://doi.org/10.1038/ncomms16075>.
- Wang, H., 2024. The role of informal ruralization within China's rapid urbanization. *Nature Cities* 1, 205–215. <https://doi.org/10.1038/s44284-024-00038-4>.
- Wilde, M., Günther, A., Reichenbach, P., Malet, J.-P., Hervás, J., 2018. Pan-European landslide susceptibility mapping: ELSUS Version 2. *J. Maps* 14, 97–104. <https://doi.org/10.1080/17445647.2018.1432511>.
- Williams, A.T., Rangel-Buitrago, N., Pranzini, E., Anfuso, G., 2018. The management of coastal erosion. *Ocean Coast Manag.* 156, 4–20. <https://doi.org/10.1016/j.ocecoaman.2017.03.022>.
- WMO, 2012. *Standardized Precipitation Index User Guide*.
- Wright, A.J., Verissimo, D., Pilfold, K., Parsons, E.C.M., Ventre, K., Cousins, J., Jefferson, R., Koldewey, H., Llewellyn, F., McKinley, E., 2015. Competitive outreach in the 21st century: why we need conservation marketing. *Ocean Coast Manag.* 115, 41–48. <https://doi.org/10.1016/j.ocecoaman.2015.06.029>.
- Yamazaki, D., Ikeshima, D., Tawatari, R., Yamaguchi, T., O'Loughlin, F., Neal, J.C., Sampson, C.C., Kanae, S., Bates, P.D., 2017. A high-accuracy map of global terrain

- elevations. *Geophys. Res. Lett.* 44, 5844–5853. <https://doi.org/10.1002/2017GL072874>.
- Yan, K., Muis, S., Irazoqui, M., Verlaan, M., 2020. Water level change indicators for the European coast from 1977 to 2100 derived from climate projections. Copernicus Clim. Change Serv. (C3S) Clim. Data Store (CDS). <https://doi.org/10.24381/cds.b6473cc1> [WWW Document].
- Zahmatkesh, Z., Karamouz, M., 2017. An uncertainty-based framework to quantifying climate change impacts on coastal flood vulnerability: case study of New York City. *Environ. Monit. Assess.* 189, 567. <https://doi.org/10.1007/s10661-017-6282-y>.
- Zscheischler, J., Westra, S., van den Hurk, B.J.J.M., Seneviratne, S.I., Ward, P.J., Pitman, A., AghaKouchak, A., Bresch, D.N., Leonard, M., Wahl, T., Zhang, X., 2018. Future climate risk from compound events. *Nat. Clim. Change* 8, 469–477. <https://doi.org/10.1038/s41558-018-0156-3>.